Published in final edited form as:
J Comp Neurol. 2004 December 20; 480(4): 392–414. doi:10.1002/cne.20359.

TrkC Kinase Expression in Distinct Subsets of Cutaneous Trigeminal Innervation and Nonneuronal Cells

Ursula Fünfschilling[1], **Yu-Gie Ng**[1], **Keling Zang**[1], **Jun-Ichi Miyazaki**[2], **Louis F. Reichardt**[1], and **Frank L. Rice**[3,*]

[1] Program in Neuroscience, Department of Physiology, Howard Hughes Medical Institute, University of California, San Francisco, San Francisco, California 94143-0723

[2] Division of Stem Cell Regulation Research, Osaka University Medical School, Osaka 565-0871, Japan

[3] Center for Neuropharmacology and Neuroscience, Albany Medical College, Albany, New York 12208

Abstract

Neurotrophin-activated receptor tyrosine kinases (Trks) regulate sensory neuron survival, differentiation, and function. To permanently mark cells that ever express TrkC-kinase, mice with *lacZ* and *GFP* reporters of Cre recombinase activity were crossed with mice having *IRES-cre* inserted into the kinase-containing exon of the TrkC gene. Prenatal reporter expression matched published locations of TrkC-expression. Postnatally, more trigeminal neurons and types of mystacial pad innervation expressed reporter than immunodetectable TrkC, indicating that some innervation transiently expresses TrkC-kinase. Reporter-tagged neurons include all those that immunolabel for TrkC, a majority for TrkB, and a small proportion for TrkA. TrkA neurons expressing TrkC-reporter range from small to large size and supply well-defined types of mystacial pad innervation. Virtually all small neurons and C-fiber innervation requires TrkA to develop, but TrkC-reporter is present in only a small proportion that uniquely innervates piloneural complexes of guard hairs and inner conical bodies of vibrissa follicle-sinus complexes. TrkC-reporter is expressed in nearly all presumptive Aδ innervation, which is all eliminated in TrkA knockouts and partially eliminated in TrkC knockouts. Many types of Aβ-fiber innervation express TrkC-reporter including all Merkel, spiny, and circumferentially oriented lanceolate endings, and some reticular and longitudinally oriented lanceolate endings. Only Merkel endings require TrkC to develop and survive, whereas the other endings require TrkA and/or TrkB. Thus, TrkC is required for the existence of some types of innervation that express TrkC, but may have different functions in others. Many types of nonneuronal cells affiliated with hair follicles and blood vessels also express TrkC-reporter but lack immunodetectable TrkC.

Indexing terms

neurotrophins; mechanoreceptors; nociceptors; IB4; CGRP; neurofilament

Trk receptors are a family of three homologous receptor tyrosine kinases TrkA, TrkB, TrkC, that are activated by the neurotrophin ligands nerve growth factor (NGF), brain-derived neurotrophic factor (BDNF), and neurotrophin-4/5 (NT-4/5), and neurotrophin-3 (NT-3), respectively. All three neurotrophins also interact with a common receptor p75NTR. The most

*Correspondence to: Frank L. Rice, Center for Neuropharmacology and Neuroscience, Room MS-538, Albany Medical College, 47 New Scotland Avenue, Albany NY 12208. E-mail: E-mail: ricef@mail.amc.edu.

prominent role of neurotrophins is to serve as target-derived neurotrophic factors for peripheral sensory and sympathetic neurons. However, all neurotrophins and their receptors serve multiple roles in the developing and mature nervous system (reviewed in Huang and Reichardt, 2001). Analysis of Trk-receptor expression patterns and of the phenotypes of knockout mice revealed that various combinations of Trk-receptors are associated with different subclasses of sensory neurons. In a very simplified view, TrkA is required mostly for small nociceptive neurons, TrkB and TrkC are required mostly for various types of cutaneous mechanosensory neurons, and TrkC is required for at least some proprioceptive neurons. There are specific examples, however, that show that some subtypes of neurons require multiple neurotrophins or trophic factors for proper development and function. Two types of sensory fibers require both TrkA and TrkC for survival: one set innervating a subset of Merkel cells in the mouse mystacial pad, the other forming a subset of peptidergic fibers innervating the epidermis (Fundin et al., 1997c; Rice et al., 1998; Cronk et al., 2002). The class of small nociceptive neurons in the dorsal root ganglia (DRG) that binds the lectin IB4 initially expresses TrkA and depends on NGF. In the late embryonic and postnatal period these neurons downregulate TrkA and switch to expression of c-ret, a common coreceptor subunit of the glial-derived neurotrophic factor (GDNF) family of ligands (Silos-Santiago et al., 1995; Bennett et al., 1996; Molliver and Snider, 1997; Molliver et al., 1997). A subset of trigeminal sensory neurons switches from BDNF to NGF-dependency in an embryonic explant or cell culture system (Enokido et al., 1999). A specialized subtype of rapidly adapting sensory neurons, the D-hair receptors, requires first NT-3 for survival but switches to NT-4 for continued survival in the adult (Stucky et al., 2002).

There are conflicting reports on the degree of coexpression of Trk receptors or the switch of expression from one receptor to another in vivo. Studies using antibody stainings in mouse found very limited coexpression of Trk receptors in the trigeminal ganglion throughout the period of gangliogenesis and no coexpression in maturing ganglia (Huang et al., 1999a). Similar studies of chicken DRGs found more extensive coexpression of TrkC with TrkA and TrkB during gangliogenesis, but also a restriction to just one Trk receptor type per cell at later stages (Rifkin et al., 2000). By in situ hybridization, extensive coexpression of TrkC with both TrkA and TrkB is detected in adult rat DRGs (Karchewski et al., 1999). Even if a neuron does not coexpress two different Trk receptors at the same time, it might switch expression from one to the other. Such a switch from TrkB and/or TrkC to TrkA is described in early trigeminal and DRG neurons (Buchman and Davies, 1993; Liebl et al., 1997). Other lines of evidence suggest that the observed shift in composition of trigeminal and dorsal root sensory ganglia from primarily TrkB/C-expressing cells to predominantly TrkA-expressing cells is due to two waves of neurogenesis in which early-born neurons express primarily TrkB or TrkC, while later-born neurons express exclusively TrkA (Enokido et al., 1999; Huang et al., 1999a). Analysis of *Ntrk* knockout animals, however, has revealed that the elimination of TrkA, TrkB, or TrkC results in 70%, 60%, and 21% reductions in neuronal numbers, respectively (summarized in Huang and Reichardt, 2001), suggesting that many neurons require more than one Trk receptor for survival during embryonic development.

To examine the extent of Trk receptor coexpression and switching, a sensitive system is required that identifies all cells that expressed a particular Trk receptor at some stage during development. In this study, we designed a cre-recombinase “knockin” strategy to focus on the expression of TrkC during and after development. In addition to the full-length, kinase-containing isoform of TrkC, two short isoforms, TrkC NC1 and TrkC NC2, are generated from the *Ntrk3* gene (Tsoulfas et al., 1993; Valenzuela et al., 1993; Menn et al., 1998). (The genes for TrkA, TrkB, and TrkC will be referred to respectively as Ntrk1, Ntrk2, and Ntrk3 according to the Mouse Genomic Nomenclature Committee, http://www.informatics.jax.org/nomen.) These short TrkC isoforms are widely expressed and might be involved in separate signaling pathways (Menn et al., 1998; Palko et al., 1999; Ichinose and Snider, 2000). The short isoforms

arise from alternative splicing, and their C-termini are encoded by separate terminal exons. Our knockin strategy was designed to restrict cre-expression to cells that only express the full-length isoform of TrkC by inserting cre-recombinase into the last coding exon of the full-length isoform using an internal ribosome entry site (IRES) and an SV40 polyadenylation site. This results in the transcription of a bicistronic mRNA from which both TrkC kinase and cre are translated. This knockin strategy guarantees that cre is strictly coexpressed with the full-length isoform of TrkC. In addition, this approach does not generate a knockout allele, but should sustain normal levels of TrkC expression. When this allele is crossed to a line that turns on a reporter gene upon cre-mediated recombination, all cells that expressed TrkC-kinase at some stage during development should be identifiable by the expression of the reporter gene.

Using this system, we found that half of the neurons in the trigeminal ganglion expressed TrkC-kinase at some stage during development. This includes all known TrkC-dependent neurons, a majority of the TrkB-dependent neurons, as well as a small, defined subset of TrkA-dependent neurons. This latter set includes relatively large neurons that supply presumptive Aδ fibers innervating the epidermis of the mystacial pad and the vasculature, as well as neurons forming some Aβ-fiber lanceolate endings. It excludes the vast majority of the C-fiber innervation. Mosaics of nonneuronal cells also expressed reporter in blood vessels and hair follicles.

MATERIALS AND METHODS

Generation of the mouse line *Ntrk3$^{tm(cre)LFR}$*

For the generation of the targeting vector, a fragment of genomic DNA containing exon 18, the last coding exon of the full-length kinase-containing isoform (Ichaso et al., 1998), was subcloned into plasmid pBluescript II KS^{-}(Stratagene, La Jolla, CA) by shotgun-cloning from a mouse bacterial artificial chromosome (BAC) clone (Incyte Genomics, Palo Alto, CA). By PCR mutagenesis, a SalI and a HindIII restriction site were inserted 52 bp behind the stop codon into exon 18 (Fig. 1A). A cassette was inserted into these restriction sites that code for cre-recombinase preceded by an internal ribosome entry site (IRES) and followed by an SV40 polyadenylation site and an FRT-site flanked neomycin resistance cassette, all derived from plasmid pSP40D (Generously provided by Ni-gel Killeen). The final targeting construct contained the pBluescript II KS-vector backbone, a 4.7 kb 5′ arm of homology, the IRES-cre-neo cassette, and a 3.4 kb 3′ arm of homology. The construct was linearized with a unique XhoI site and transfected into embryonic stem cells using standard techniques. Of two stem cell lines that contained the correct targeted locus as assayed by Southern blot and PCR, one line generated chimeras with germline transmission. To eliminate the FRT-site flanked neo-cassette, mice were crossed to a FLPe deleter strain (Rodriguez et al., 2000). Correct excision of the neo-cassette was confirmed by Southern blot and PCR. The line was maintained on a C57/Bl6 wildtype mouse genetic background, but the reporter mouse lines are on a mixed genetic background. Primers 2 (TCCTCCATGCTTTGGGGAAGGC-CAC) and 3 (TGCCGCCTTTGCAGGTGTGTCTTAC) amplify a 407-bp band from the targeted locus, primers 2 and 4 (CAGTGTTGTATGTGTAGCAGGCACT) a 204-bp band from the wildtype locus (TRKC2B-F and TRKC2-R also amplify a 2,256 bp band from the targeted locus which is usually only detected in homozygous animals). Primers 1 (AGGTGAGTAGGTCTTCTTGTAGTGTAATTG) and 5 (AAAGGACCATCAAGTTCACATTCAAAGCAA) amplify an 8.3 kb band from the wild type locus, and a 10.3 kb band from the targeted locus. The expression pattern of cre was analyzed in the offspring of crosses between homozygous *Ntrk3$^{tm(cre)LFR}$* animals and homozygous R26R or heterozygous CAG-CAT-EGFP (GFP) reporter mouse lines (Soriano, 1999; Kawamoto et al., 2000). All analyzed animals were thus heterozygous for both the cre and the reporter locus.

Northern

Total brain RNA was isolated using RNA-Bee (Tel-Test, Friendswood TX; CS-104B), subsequently poly-A+ RNA was isolated using Oligotex beads (Qiagen, Chatsworth, CA; 70022), and the RNA was transferred to Hybond-N+ (Amersham, Arlington Heights, IL; RPN 303B). Hybridizations were done in Rapid-Hyb buffer (Amersham RPN 1636) using redi-primeII (Amersham RPN 1634). The TrkC kinase probe was cut from pCMX-rTrkC (Tsoulfas et al., 1993) with ApaI. The TrkC extracellular probe was cut from pLL63 (generously provided by M. Barbacid) with HindIII. The IRES-cre probe was cut from pSP40D (generously provided by Nigel Killeen) with EcoRI-SalI.

Histological analysis

All animals were treated according to the NIH guidelines for animal care using protocols accepted by the UCSF committee on animal health. Embryos were fixed in 4% paraformaldehyde (PFA) in phosphate-buffered saline (PBS) at pH 7.4. Adult animals were deeply anesthetized with avertin (2.5% in PBS) with 20 μl per gram body weight and were pericardially perfused with 20 ml of PBS, 50 ml of 4% PFA in PBS. Dissected tissues were postfixed for 30 minutes to 4 hours in 4% PFA, cryoprotected in 30% sucrose in PBS, cut on a cryostat, and stained according to standard procedures (Rice et al., 1997). Mystacial pads were cut in 14-μm-thick sections oriented perpendicular to the skin surface and parallel to the rows of vibrissa follicles. Primary antibodies/lectins consisted of rabbit-anti-GFP (plain or conjugated to AlexaFluor 488, Molecular Probes, Eugene, OR; A-11122 and A-21311), rabbit-anti-150kD and anti-200kD neurofilament proteins (NF150, NF200; Chemicon, Temecula, CA; AB1981, AB1982), rabbit-anti-protein gene product 9.5 (PGP; UltraClone, Isle of Wight, UK), guinea pig and rabbit anti-calcitonin gene-related peptide (CGRP; Peninsula, Belmont CA; T-5027 and T-4032), rabbit-anti-β-galactosidase (β-gal; 5 Prime-3 Prime, Boulder CO; 7-06310), mouse-anti-β-gal (Promega, Madison, WI; Z3781), rabbit-anti-TrkA (Clary et al., 1994), rabbit-anti-TrkB, goat-anti-TrkC (Huang et al., 1999a), and FITZ-conjugated lectin BS-I (a lectin containing isolectin IB4; Sigma, St. Louis, MO; C-2895). Appropriate species of secondary antibodies were conjugated to either Cy3 or Cy2 (Jackson ImmunoResearch Laboratories, West Grove, PA) or AlexaFluor 488 (Molecular Probes). Staining for β-gal with X-Gal was done at 37°C (10 mM Tris-Cl, pH 7.3, 1 mg/ml X-Gal (Roche, Nutley, NJ; 745740), 0.01% Na-Desoxycholate, 0.02% Nonident P-40, 4% dimethylformamide, 2 mM $MgCl_2$, 1 mM $K_3Fe(CN)_6$, 1 mM $K_4Fe(CN)_6$), counterstaining with Fast Nuclear Red (Vector Laboratories, Burlingame, CA; H-3403). Double labels involving rabbit primary antibodies in combination with rabbit-anti-GFP were done sequentially using Cy3-conjugated F_{ab} fragments (Jackson ImmunoResearch, 11-167-003) to detect the first rabbit antibody, followed by rabbit-anti-GFP directly conjugated to the fluorophore AlexaFluor 488.

Images of ganglion sections were captured on a digital SPOT camera (Diagnostic Instruments, Sterling Heights, MI; RT Slider 2.3.1) on a Nikon Eclipse E600 microscope using a 10× or 40× air objective, manually assembled into complete montages using the software Canvas (Deneba, ACD Systems). Images of mystacial pad sections were captured on an Olympus Provis AX70 epifluorescence microscope (Cy-3 filters: 528 –553 nm excitation, 590 – 650 nm emission; Cy-2 and AlexaFluor 488 filters: 460 –500 nm excitation, 510 –560 nm emission) equipped with a high-resolution three-color CCD camera (Sony, DKC-ST5) interfaced with Northern Eclipse software (Empix Imaging, Mississauga, ON). Double labeling was assessed by digitally merging the red and green signals, then alternatingly phasing in and out the separate signals. To control for nonspecific labeling, incubations were conducted without the primary antibodies or with primary antibodies preabsorbed with their specific blocking peptide. To control for false-positives due to cross binding in double-label combinations, the order of the primary antibody incubations was reversed for each double-label combination. All permutations of double labeling were conducted that would test for coexpression of antigens

and that would control for, and rule out nonspecific labeling on the innervation. Furthermore, the order of Cy-3 and Cy-2 or AlexaFluor 488 conjugated secondary antibodies was also reversed to control for nonspecific labeling among secondary antibodies and for any "bleeding" of Cy-3 fluorescence through the Cy-2/AlexaFluor 488 filters or vice versa.

The immunofluorescence results are based on what was originally observed on the slides and digitally captured images without any manipulation. Since background fluorescence as determined from control sections is useful for identifying unlabeled structures, the contrast and brightness of the digital images was purposefully manipulated as little as possible to maintain the true appearance of the sections and the range of labeling intensities while qualitatively balancing the relative maximum intensities of the red and green signals. Therefore, when the maximum intensity in one color channel is relatively low or the range of labeling intensities is relatively narrow compared to the other channel, the balancing of the maximum intensity for publication purposes can artifactually enhance what is truly background labeling. In most mystacial pad sections, the endogenous green GFP fluorescence was enhanced by incubating with anti-GFP followed by AlexaFluor 488 secondary antibody. In a few cases, the anti-GFP was purposefully labeled with Cy3. In these few cases, the red and green channels in the digital images were usually reversed so that GFP labeling is shown in the green channel. In all of the figures, red and green symbols are used to indicate innervation that is only labeled by one antibody, and yellow to indicate double-labeled innervation. In many figures, the red, green, and merged images are individually shown in order to document the most important but sometimes subtly different or similar results. In some figures of lesser importance, only the merged images are shown, even though the double-labeling (as determined from viewing the separate channels) may not be obvious due to differences in the relative intensities of signals among the variety of total structures within the images.

Cell counts and morphometry

For cell counts and morphometric analyses, one ganglion each from at least three different animals was analyzed per time point. In all counts, entire cross sections of the ganglion were analyzed and only cells containing a nucleus were scored. For embryos, three sections equally spaced apart and spanning the entire length of the ganglion were chosen, corresponding to 1,000 –2,500 cells per animal. For postnatal animals, four to six sections equally spaced apart and spanning the entire length of the ganglion were scored. For adult cell size measurements in sections stained for TrkA and GFP, six or seven sections equally spaced apart and spanning the entire length of the ganglion were analyzed, resulting in the analysis of more than 1,000 cells per animal. Neurons negative for both TrkA and GFP were identified by their morphology in the faint fluorescence that was regarded as background based on comparison to unlabeled control sections in wildtype mice. Cells were counted and measured using the free software ImageJ (available from http://rsb.info.nih.gov/ij/). For the double-label analyses where only a relative percentage of labeled cells was determined (TrkB, CGRP, and IB4 versus GFP), all strongly marker-positive cells were marked in an entire section in the red channel and, subsequently, the GFP-positive subfraction of the marked neurons was determined by analysis of the green (GFP) channel.

Birthdate analysis

Females were put together with the males around 5 PM and, if a vaginal plug was discovered the next morning, the female was considered pregnant day zero (E0). Pregnant females were injected intraperitoneally with 50 mg/kg BrdU from a 10 mg/ml BrdU solution in PBS (5-Bromo-2′-deoxyuridine, Sigma B-9285) at noon of embryonic day 9.5 (E9.5) or 11.5 (E11.5). Pups were harvested at birth and processed for immunohistochemistry as described above. For triple-labels against β-gal, TrkA, and BrdU, sections were first stained with biotinylated mouse-anti-β-gal (antibody from Promega: Z-3781, biotinylated with EZ-Link Sulfo-NHS-LC-Biotin

according to the manufacturer's instructions (Pierce, Rockford, IL; 21338)), followed by detection with streptavidin-Alexa Fluor488 (Molecular Probes S-11223), fixed 5 minutes in 4% PFA in PBS on ice, "unmasked" 30 minutes in 2 M HCl at 37°C, neutralized 10 minutes in 0.1 M borax, and processed for regular immunohistochemistry with rabbit-anti-TrkA (Clary et al., 1994) and mouse-anti-BrdU (Pharmingen, San Diego, CA; 555627) detected by donkey-antirabbit-Cy3 and donkey-antimouse-Cy5 (Jackson ImmunoResearch, 711-165-152 and 715-175-150). Random pictures of the ganglia were taken on an MRC 1000 confocal microscope (Bio-Rad, Hercules, CA) using a 63× oil objective and all cells in the frame were analyzed using the free software ImageJ based on 260 –700 cells per animal.

RESULTS

Generation of the mouse line *Ntrk3$^{tm(cre)LFR}$*

To knock cre recombinase into the *Ntrk3* locus, a targeting construct was generated (Fig. 1) and transfected into embryonic stem cells. Chimeras were generated from two stem cell lines, and germline transmission was obtained from one line. To minimize disturbance of the genomic locus, the neomycin resistance gene was removed by FlpE-mediated recombination (Rodriguez et al., 2000). Correct integration and removal of the selection cassette was confirmed by Southern blot, as well as by PCR across the entire targeted region (Fig. 1B, C, and data not shown). The mice appeared healthy and were viable and fertile as homozygous animals, indicating that expression of TrkC was not disturbed. Analysis of Northern blots from polyA + RNA from total brain confirmed that the wildtype transcript encoding the full-length isoform was reduced by 50% in the heterozygous animals and that one major new, shorter transcript appeared that was recognized by probes against the extracellular domain, the kinase domain and the IRES-cre, confirming that a new bicistronic transcript was formed (Fig. 1D). In homozygous animals, the new transcript fully replaced the original full-length isoform. The transcripts coding for the truncated isoforms were not affected. The slight increase of the signal at the position of the truncated isoforms in the heterozygous and homozygous animals seems to be due to the signal of the partially overlapping new transcript. The new transcript was smaller than the original full-length mRNA despite the insertion of a 2 kb IRES-cre-pA cassette. This indicates that the wildtype transcript contains a very long 3′-untranslated region, which is truncated by the insertion of a SV40 polyadenylation site right after cre. To mitigate any effect that this alteration of the mRNA could have on the TrkC expression, we performed the entire analysis on a heterozygous background.

Analysis of the mouse line *Ntrk3$^{tm(cre)LFR}$*

To analyze the expression pattern of cre, we crossed *Ntrk3$^{tm(cre)LFR}$* to the R26R reporter line, which constitutively activates the transcription of β-gal upon cre-mediated recombination (Soriano, 1999). Once recombination occurs, β-gal is expressed independently of cre, and the activated allele is also transmitted to the progeny of proliferating cells. At low magnification (Fig. 2A), the observed pattern of β-gal expression in the developing embryo was comparable to the published expression pattern of TrkC (Tessarollo et al., 1993; Lamballe et al., 1994). Scattered cells were detected as early as E10.5. By E17.5, β-gal was observed in the brain, in sensory neurons, along nerves, in the sympathetic nervous system, as well as outside the nervous system in the submandibular gland, major blood vessels, kidney, muscles, and connective tissue (Fig. 2A, and data not shown). A detailed analysis at the cellular level was carried out in the trigeminal ganglion, the superior cervical ganglion, and the mystacial pad as discussed below. At E14.5, all trigeminal sensory neurons that stained with an antibody against TrkC also stained for β-gal (data not shown), further confirming the correct targeting of the *Ntrk3* locus.

Time course of reporter expression in the trigeminal ganglion

Further analysis focused on the trigeminal ganglion, which contains the sensory neurons that innervate the face, including the mystacial pad. For the initial characterization we used the R26R reporter mouse because it is the most sensitive reporter line in our hands. The first recombined neurons in the trigeminal ganglion were detected at E11.5. The percentage of recombined cells rapidly increased and reached a plateau around 50% recombination after birth (Fig. 3A). This contrasts with previous studies that found that only about 10% of the trigeminal neurons express TrkC at E13.5 or birth, based on antibody staining or in situ hybridization (Liebl et al., 1997;Huang et al., 1999a), and only 20 –30% of the neurons require TrkC for survival (Piñon et al., 1996;Liebl et al., 1997). Our data thus indicate that more trigeminal neurons express TrkC kinase at some stage during development than previously suspected.

A similar time course was obtained with a different reporter mouse line, CAT-CAG-EGFP, which expresses GFP upon cre-mediated recombination (Kawamoto et al., 2000). This reporter allele appears to be less sensitive than the R26R line to cre-mediated recombination and showed a slower rise and a lower plateau value of 40% of recombination (Fig. 3A). Immunolabeling of mystacial pads in R26R and CAT-CAG-EGFP lines revealed identical expressions of β-gal and GFP in nonneuronal cells and in large nerves and sensory endings of large caliber axons (Figs. 2C, D, 6A, B, 11). β-Gal may not have diffused completely in most small-caliber innervation (Rico et al., 2002) and was usually not detected in their endings (Figs. 6B, 7A, B). Therefore, detailed analyses of the mystacial pad innervation were conducted mostly on the CAT-CAG-EGFP reporter line because GFP apparently diffuses better throughout the neurons, marking even terminal arbors of small fibers. All sites of innervation were comparable to those in wildtype mice.

Marker expression in the trigeminal ganglion

Since the expression of Trks can change and typically decrease during development in many sensory neurons, we assessed some of this dynamic by comparing which populations of trigeminal sensory neurons coexpressed the GFP reporter with various Trk and other immunoand histochemical labeling in 2-day-old mice (P2) and in adults (7 weeks). The data are summarized in Table 1. Although endogenous GFP fluorescence was detectable both in cell bodies and in fine terminal nerve endings, we routinely used anti-GFP to enhance the signal. At P2, 57% of the strongly TrkB-expressing neurons coexpressed GFP, indicating that TrkB cells preferentially coexpress TrkC kinase at some stage during embryonic development. At 7 weeks, 70% of the TrkB-expressing neurons coexpressed GFP. In contrast, only 9% of the TrkA-expressing neurons coexpressed GFP at P2. In accordance with published results, the percentage of all TrkA-expressing neurons decreases by about half (42% to 21%) between P2 and adulthood (Table 1). Of the remaining TrkA-expressing neurons in adults, 19% coexpressed GFP. The total number of neurons in the ganglion did not change significantly (3.7– 4.0%) from P2 to adulthood, indicating that many of the GFP-negative neurons most likely downregulated TrkA. Consistent with this likelihood and the observation that small IB4-binding neurons downregulate TrkA in developing dorsal root ganglia (Silos-Santiago et al., 1995;Bennett et al., 1996;Molliver and Snider, 1997;Molliver et al., 1997), only 11% of the IB4-binding neurons in the trigeminal ganglion coexpressed GFP, indicating that the vast majority never express TrkC kinase. Most of the likely IB4-related C-fiber innervation in the mystacial pads also lacked GFP. The presence of CGRP designates peptidergic sensory neurons. We found that 16% of the CGRP-positive neurons coexpressed GFP, which correlated well with the analysis of peripheral innervation (see below).

Size distributions and birthdates of TrkA-and GFP-expressing neurons

Analyses of trigeminal ganglia at 7 weeks revealed that neurons expressing either GFP or TrkA spanned a comparably broad range of sizes, but the distribution of the GFP-expressing cells

was shifted towards larger sizes while that of TrkA-expressing cells was shifted towards smaller sizes (Fig. 3B). This is in good agreement with published results showing that TrkA neurons are generally smaller and are the source mostly of C fibers and Aδ fibers. TrkC and TrkB-expressing neurons (which make up the majority of the GFP-expressing cells) are generally larger and are typically the source of faster-conducting Aδ and Aβ fibers (Mu et al., 1993). Interestingly, neurons that coexpressed TrkA and GFP at P2 or in the adult had relatively large sizes, on average even larger than that of the GFP-only expressing cells (Figs. 2B, 3C, and data not shown). This is again consistent with the likelihood that the very small, IB4-binding neurons preferentially do not express GFP. The broad size distribution of the TrkA-GFP double-labeled cells suggests that they constitute a heterogeneous population of neurons. Consistent with this indication, GFP was detected in specific subsets of C, Aδ, and Aβ fibers that are known to depend on TrkA in the developing mystacial pad.

Previous work has shown that trigeminal neurons are born in two overlapping waves, with neurons of the first wave (E9.5) expressing primarily TrkC or TrkB, while neurons in the second wave (E11.5) express exclusively TrkA (Enokido et al., 1999; Huang et al., 1999a). We used BrdU (5-Bromo-2′-deoxyuridine) injections in pregnant dams from crosses of *Ntrk3*$^{tm(cre)LFR}$ to R26R animals to label early-born and late-born neurons. Subsequently, we tested at P2 for colabeling between BrdU, β-gal, and TrkA. Consistent with the published results, we found that 54 ± 6% (mean ± STD) of the β-gal-positive neurons (presumed TrkC and many TrkB neurons) were born early, around E9.5, compared to only 21 ± 5% born around E11.5. In a slight deviation from published results, we found similar percentages of TrkA neurons born in both waves: 42% mean ± 18% STD at E9.5 and 38% ± 8% at E11.5. The unexpectedly high proportion of TrkA cells “born” at E9.5 might be an overestimate due to the low cutoff that was used to score BrdU-positive nuclei, so some nuclei might have been included that still had divided after incorporation of the BrdU label. The birthdates of the TrkA/β-gal coexpressing neurons were distributed similarly between the two waves: 50 ± 8% born at E9.5 and 41 ± 6% at E11.5. This may indicate that the phenotype of TrkA cells does not strongly depend on the birthdate of the neuron, or it may reflect the heterogeneous mixture of TrkA cells that coexpress GFP as indicated by the wide cell body size distribution.

Analysis of the mystacial pad

To further analyze the neuronal subtypes that express reporter in the trigeminal ganglion, we analyzed the peripheral innervation of the mystacial pad, the major target of the trigeminal nerve in the mouse. Unless indicated otherwise, most of the documentation is from the CAT-CAG-EGFP reporter line. As shown schematically in Figure 4, the mystacial pad is densely innervated by a variety of morphologically and histologically distinguishable nerve endings that all label with anti-PGP (Rice et al., 1993,1997;Fundin et al., 1994). The various sensory endings are supplied by a mix of Aβ, Aδ, and C fibers. Previous studies have shown which of these nerve endings depend on TrkA, TrkB, TrkC, and p75NTR (Fundin et al., 1997c;Rice et al., 1998). Our results are summarized and compiled with results from other studies in Figure 5.

Nonneuronal cell types

In addition to GFP-label in nerve fibers, we found abundant GFP expression in nonneuronal tissues, which is consistent with published results (Tessarollo et al., 1993; Lamballe et al., 1994) and with the results observed in the R26R reporter mouse (e.g., Figs. 2A, C, D, 6A, B, 11). GFP was expressed in many keratinocytes of virtually all hair follicles but was rarely present within keratinocytes in the epidermis (Figs. 4, 7). Detectable GFP was limited to specific sites within the follicles. Among the intervibrissa hairs, GFP was only observed in the bulbs at the deep end of the follicles (Fig. 4D). Although vibrissa follicles also have GFP-positive cells at the level of the follicle bulbs, GFP expression was most intense and most

widespread in keratinocytes at upper cavernous sinus and lower ring sinus levels, then tapered to the keratinocytes near the core of the follicle at the level of the upper ring sinus and extended up to and included a mosaic of keratinocytes in the epidermis at the rete ridge (Fig. 4A–C). GFP was conspicuously absent among keratinocytes in the vicinity where sensory endings (Merkel endings) terminate on Merkel cells in the outer root sheath at the level of the ring sinus (Figs. 4A, C, 11). These distributions of the GFP-positive keratinocytes suggest that the follicles are heterogeneous structures and that the stem cells that regenerate the hair follicle during turnover are GFP-negative and, thus, have never expressed TrkC kinase.

Other sites of GFP-expression included smooth muscles cells (both piloerector and vascular tunica media), presumptive endothelial cells, and fat cells (Fig. 6). An unusual cell type with a “dendritic” morphology was also labeled in the tunica adventitia of blood vessels (Fig. 6D). GFP-expression was mosaic, with positive and negative cells intermixed. Although this suggests that there may be an unsuspected developmental heterogeneity among these nonneuronal cells, it may alternatively reflect low “transcriptional noise” of the *Ntrk3* promoter. Interestingly, the endogenous GFP-fluorescence was exceptionally intense in hair follicle cells compared to that in the other nonneuronal cell types. Heterogeneity in GFP levels was also observed in the trigeminal ganglion (Fig. 2B). The heterogeneity of GFP-expression levels was independent of the expression level of TrkC kinase, but presumably reflects cell-specific differences in reporter protein stability or in transcription of the reporter from the randomly integrated transgene. Importantly, none of the GFP-positive nonneuronal cells labeled with anti-TrkC, at least after the fourth postnatal week. This indicates that TrkC kinase was expressed in these nonneuronal cells during development, but is no longer expressed in these same cells in the adult.

Schwann cells

GFP was expressed in Schwann cells in both the trigeminal ganglion and the periphery (Fig. 2B–E). Virtually all of the Schwann cells in the trigeminal motor nerve (Fig. 2B) and on branches of the facial motor nerve innervating facial muscles were GFP-positive. In contrast, branches of the trigeminal sensory nerves contained a heterogeneous mix of reporter-negative and reporter-positive Schwann cells (Fig. 2C–E). The entire lengths of individual axons that could be observed in a section appeared to be lined by either GFP-positive or GFP-negative Schwann cells. This suggests that clonal populations of Schwann cells remain associated with single axons at least across several internodes. GFP-positive Schwann cells were found on axons of all calibers and were not preferentially associated with GFP-positive axons. Although GFP-expression in Schwann cells made it more difficult to detect GFP within axons and endings, this was mostly resolved through double-labeling with anti-PGP, anti-NF200, or anti-CGRP, which are preferentially or entirely expressed within axons. The Aβ fibers that supply club endings at the level of the ringwulst in FSCs provide an example where GFP-negative axons can be covered by GFP-positive Schwann cells (Fig. 12D). The GFP-negative club-endings clearly protrude beyond the GFP-positive Schwann cells investing the axon. As was the case with other nonneuronal cells, Schwann cells in 4-week postnatal animals do not label with anti-TrkC, indicating that the TrkC kinase was primarily expressed earlier during development.

Epidermal and upper dermal innervation

Labeling with anti-PGP revealed that the epidermis and upper dermis is innervated almost entirely by thin caliber axons (Fig. 7). Labeling with anti-NF200 revealed that most of these axons are NF200-negative but a substantial proportion are NF200-positive (Figs. 4, 7A, D). Prior studies in other species have detected that NF200 and myelin basic protein are consistently coexpressed and that this coexpression occurs on all thick caliber axons which are Aβ fibers, and some thin caliber axons which are presumptive Aδ fibers (Fundin et al.,

1997b,c;Rice et al., 1997;Paré et al., 2001). Thin NF200-negative axons are presumptive unmyelinated C fibers. Unfortunately, the most reliable antibody that we have found against myelin basic protein is raised in mice (Sternberger Monoclonals, Baltimore, MD) but we have been unable to obtain enough signal to background labeling in mouse skin to reveal the thin myelin sheaths that we have detected on presumptive Aδ fibers in other species.

Double-label combinations with antibodies against anti-PGP, anti-NF200, and anti-GFP revealed that virtually all of the presumptive Aδ innervation (thin caliber, NF200-positive) coexpressed GFP in CAT-CAG-EGFP mice (Fig. 7D). Comparing the two reporter lines, β-gal was not as well detected as GFP among the upper dermal innervation and only GFP reporter could be unequivocally detected in the epidermis (Fig. 7A, B). Compared to the total upper dermal and epidermal innervation seen with anti-PGP, most of the presumptive C fiber innervation (thin caliber NF200-negative) innervation lacked GFP (Fig. 7A, D). Only a few thin caliber axons were NF200-negative and GFP-positive (Fig. 7D). In prior studies, the presence of virtually all presumptive C and Aδ fiber innervation throughout mystacial pads has been shown to depend on TrkA (Rice et al., 1998). Our current results indicate that the Aδ innervation to the upper dermis and epidermis also expresses TrkC kinase at some point during development (Figs. 5, 7D). Although TrkA-immunolabeling was detected among a large proportion of thin fibers, and TrkC on a smaller proportion of thin caliber fibers in mystacial pads on P2 (Figs. 7F, G), little TrkA and no TrkC-immunolabeling was evident on such fibers 7 weeks after birth (data not shown).

Previous studies demonstrated that CGRP-IR is detectable on a sizeable minority of the epidermal and upper dermal innervation, and that a subpopulation of this peptidergic innervation coexpresses NF200-IR (Fundin et al., 1997a; Rice et al., 1998). Most of the CGRP-positive innervation lacked GFP as well as NF200, whereas GFP was coexpressed on CGRP-positive innervation that contained NF200 (Fig. 7C, D). These results indicate that the TrkC kinase-expressing Aδ innervation includes peptidergic (CGRP-positive) and nonpeptidergic (CGRP-negative) innervation (Fig. 5).

Sensory and sympathetic innervation of blood vessels

Previous studies have shown that arterioles in the mystacial pad are innervated by sympathetic fibers intimately associated with the tunica adventitia-tunica media border, as well as sensory fibers located more peripherally in the tunica adventitia (Fundin et al., 1997b). Double-labeling to detect PGP and GFP revealed that none of the sympathetic innervation expressed detectable GFP (Fig. 8B). Our analysis of the superior cervical ganglion, the source of the sympathetic innervation of the mystacial pad, revealed that only 26 ± 10% (n = 3) of the sympathetic neurons expressed GFP, with many of these cells expressing very low levels of GFP. Thus, the vascular sympathetic innervation to the mystacial pad may be supplied from the subpopulation of sympathetic neurons that do not express TrkC kinase at any stage during development (Fig. 5).

Consistent with prior observations in the rat (Fundin et al., 1997b), we found that the entire sensory innervation of the vasculature expresses CGRP, and consists mostly of NF200-negative presumptive C fibers plus a smaller proportion of NF200-positive presumptive Aδ fibers (Fig. 8B–D). GFP was consistently expressed only in the Aδ peptidergic fibers (Fig. 8B–D). Although all of the vascular innervation has been shown to depend on TrkA during development (Fundin et al., 1997b; Rice et al., 1998), at 7 weeks TrkA-immunolabeling was only detected on the vascular innervation that coexpressed NF200 and GFP, indicating that it was limited to the Aδ innervation (insert in Fig. 8D). Thus, the presumptive Aδ vascular innervation may originate from the small- to medium-sized neurons that coexpress TrkA, CGRP and GFP in mature trigeminal ganglia (Table 1; Fig. 5). None of the vascular innervation labeled as well with β-gal as with GFP reporter (Fig. 6A, B).

Circumferentially oriented hair follicle innervation

Prior studies revealed several types of intermingled endings that were circumferentially oriented and were in two locations: 1) as part of the piloneural complexes (PNCs) surrounding guard hair follicles (Figs. 4, 9) just below the sebaceous gland; and 2) in the inner conical bodies (ICBs) surrounding the upper end of vibrissa follicles (Figs. 4, 10) (Fundin et al., 1997a,c;Rice et al., 1997,1998). As was seen previously in the rat, our results in the mouse demonstrate that this circumferential innervation in both locations consists of at least three types (Figs. 9,10). One type is a presumptive peptidergic C-fiber innervation that has a thin caliber and is CGRP-positive and NF200-negative. The second type is a presumptive non-peptidergic C-fiber innervation that has a thin caliber and is only detected with anti-PGP, therefore lacking CGRP or NF200. The third type is a medium caliber Aβ-fiber innervation that is CGRP-negative and NF200-positive and forms circumferentially oriented lanceolate endings (Mosconi et al., 1993). Importantly, previous research has shown that all of the circumferentially oriented endings in the ICBs and PNCs are completely absent in both *NGF* and *Ntrk1* knockouts and that much of the innervation still remains in *Ntrk2* or *Ntrk3* knockouts (Fundin et al., 1997c). However, the remaining endings in the *Ntrk2* or *Ntrk3* mutants were not further characterized in that study (Fig. 5).

Our results revealed that all of the NF200-positive circumferential innervation, i.e., the Aβ, in the ICBs and PNCs expressed GFP (Figs. 9D, 10C). β-Gal could not be as reliably detected in this location as GFP. Since this innervation is lost in the *Ntrk1* knockout, the circumferential lanceolate innervation must express both TrkA and TrkC kinase during development, but not necessarily at the same time. We detected TrkA immunoreactivity on circumferential lanceolate endings in mature ICBs (insert in Fig. 10C), indicating that these medium-caliber Aβ fibers (Munger and Rice, 1986;Rice et al., 1998) are very likely derived from the medium-size TrkA-expressing, GFP-positive neurons observed in the postnatal trigeminal ganglion (Table 1, Fig. 5).

Our results also reveal that none of the circumferential CGRP-positive C-fiber innervation coexpressed GFP, although these peptidergic fibers were intermingled with GFP-positive/CGRP-negative fibers (Figs. 9C, 10B). Thus, the peptidergic C-fiber innervation may depend on TrkA but not TrkC, although we were unable to detect TrkA-IR on this innervation in mature mystacial pads. In contrast, GFP was expressed on at least some of the nonpeptidergic C-fiber innervation in PNCs as well as in ICBs (Figs. 9D, 10C), indicating that this innervation may be dependent on TrkA and TrkC. However, no TrkA or TrkC immunoreactivity was detected in the adult on this innervation either (Fig. 5). Importantly, much of this nonpeptidergic C-fiber innervation in the rat labels with IB4 (Fundin et al., 1997c;Rice et al., 1997). Consequently, this innervation may account for the presence of the small percentage of GFP expressing IB4 neurons in the trigeminal ganglion (Table 1, Fig. 5). Unfortunately, IB4 labels the surface of nearly all nerves as well as a variety of other structures in mouse mystacial pads, making it too nonspecific to interpret (Rice, unpubl.).

Merkel innervation

Merkel innervation is supplied by the largest caliber Aβ fibers which penetrate the basement membrane, then branch and terminate on specialized Merkel cells in the outer root sheath at the ring sinus level, in the rete ridge of vibrissa follicles (Figs. 4, 11), as well as in the outer root sheath of some large guard hairs (Figs. 4, 9B, C). All of the Merkel innervation expressed β-gal and GFP reporter and also labeled with anti-TrkC as well as anti-TrkB at 7 weeks (Figs. 9B, C; 11). Thus, this innervation probably arises from some of the large neurons that coexpress reporter and TrkB in the trigeminal ganglion (Table 1, Fig. 5). Consistent with these results, previous studies have shown that Merkel endings are heavily dependent on TrkC for their survival and on TrkB for their function, although some Merkel endings also appear to have a

transient dependency on TrkA (Fundin et al., 1997b;Cronk et al., 2002). The Merkel cells that the endings terminate upon express immuno-reactivity for PGP and CGRP but have little if any GFP, indicating that they may have never expressed TrkC kinase (Fig. 9B, C).

Longitudinal lanceolate endings

Longitudinal lanceolate endings are fork-like endings supplied by medium-caliber Aβ fibers, and are located in the mesenchymal sheath at the ring sinus level of vibrissa follicles and around guard hair follicles just below the sebaceous glands (Fig. 4). Collectively, they form a more or less complete palisade around a given follicle. Multiple axons supply endings to each palisade. Around vibrissa follicles, some of the Aβ fibers can terminate as just two or three exceptionally long, widely spaced endings, whereas others terminate as several short, tightly clustered endings (Fig. 12A–C) (Fundin et al., 1995). Around guard hair follicles, the longitudinal lanceolate endings have a much shorter, generally uniform length (Fig. 9A–C).

We found that only the long type of mature vibrissa lanceolate endings expressed TrkA-immunoreactivity (Fig. 12B), whereas all types expressed TrkB (Figs. 5, 12C). Around mature guard hair follicles, none expressed detectable TrkA-immunolabeling and only some labeled with anti-TrkB (Fig. 9B). Most if not all of the longitudinal lanceolate around mature vibrissa follicles expressed GFP (Figs. 5, 12A) or β-gal (not shown). Only GFP was reliably detected among longitudinal lanceolate endings around guard hair follicles, but this expression was variable from follicle to follicle, ranging from a few endings to virtually all endings of a given palisade (Fig. 9A–C). However, no TrkC immunoreactivity was detected on any mature lanceolate endings (Fig. 5). Around guard hairs, TrkB-immunolabeling on the lanceolate endings did not consistently correlate with GFP expression: i.e., GFP-positive endings could be TrkB-positive or -negative, and TrkB-positive endings could be GFP-positive or -negative. Taken together, these results suggest that longitudinal lanceolate innervation appears to be heterogeneous and may account for many of the medium to large adult neurons that may express reporter and TrkA and/or TrkB.

Club endings

A recent confocal analysis (Ebara et al., 2002) revealed the presence of a previously overlooked set of large caliber Aβ fibers that each terminate as one or two morphologically simple club-like endings (Figs. 4, 12D). The population of club endings are evenly spaced and are located precisely at the attachment of a donut-shaped structure (the ringwulst) around the perimeter the mesenchymal sheath at the middle of the vibrissa follicles. The club endings did not express detectable amounts of GFP or β-gal (Fig. 12D, and data not shown), indicating that they never express or depend on TrkC kinase during development. However, some reporter was consistently expressed in their myelin sheaths. These club endings were also not labeled with anti-TrkA, TrkB, or TrkC (Table 1, Fig. 5). Although the impact of trophin-related knockouts was not assessed on these previously overlooked endings, retrospective examination of published micrographs confirmed that club endings were not affected, at least in *Ntrk3* knockouts (see fig. 6D in Fundin et al., 1997c).

Reticular and spiny (Ruffini) endings

Previous assessments of vibrissa FSC innervation revealed the presence of two types of Aβ-fiber endings that terminate in the mesenchymal sheath around the follicle at the level where trabeculae span the lumen of the cavernous sinus (Fig. 4). Medium-to-large caliber Aβ fibers supply highly branched, interdigitating reticular endings that are densely packed against the basement membrane of the follicle. Fewer, slightly larger caliber Aβ fibers supply less branched and segregated spiny endings that terminate slightly displaced from the basement membrane (Ebara et al., 2002). Spiny endings had previously been erroneously designated as “Ruffini endings” (Fundin et al., 1997c).

Previous studies indicated that the reticular endings are virtually eliminated in both *NGF* and *Ntrk1* knockouts but are increased in *Ntrk3* knockouts (Fundin et al., 1997c). We found no TrkA immunoreactivity on any reticular endings in this location in mature animals, indicating that TrkA must be expressed on these neurons at an earlier stage in development. However, many, but not all, of the mature reticular endings expressed both GFP and TrkC immunoreactivity (Fig. 12E). Comparable labeling was obtained with the β-gal reporter (not shown). These results indicate that reticular endings may also be heterogeneous and are supplied by medium to large caliber neurons that can either lack GFP and TrkC or coexpress both GFP and TrkC (Fig. 5).

Previous work has shown that the presence of spiny endings depends only on TrkB and BDNF (Fundin et al., 1997c). Consistent with this, the spiny endings expressed TrkB, but not TrkA at maturity (Fig. 12E). These endings also consistently expressed GFP or β-gal and TrkC-immunoreactivity (Fig. 12E). These results indicate that mature spiny endings originate from trigeminal neurons that coexpress TrkB and TrkC (Fig. 5).

DISCUSSION

Analysis of the mouse line *Ntrk3$^{tm(cre)LFR}$*

The family of the Trk receptors TrkA, TrkB, and TrkC are required for the survival and differentiation of most sensory neurons, with each receptor being important for a specific subset of neurons (summarized in Fig. 5). To test whether there is significant switching and/or coexpression of Trk receptors during development of sensory neurons, we developed a genetic system that allows the identification of all neurons that have expressed TrkC kinase at any time. To this end, we generated a “knockin” mouse that expresses cre-recombinase from a bicistronic mRNA together with the full-length kinase-containing isoform of TrkC. We crossed this mouse line to β-gal and GFP reporter lines and compared reporter expression to the published patterns of TrkC expression. The most extensive expression analyses were previously done with probes or antibodies recognizing the extracellular domain of TrkC, thus recognizing all isoforms, including those lacking a kinase domain (Tessarollo et al., 1993;Lamballe et al., 1994). At low magnification, our reporter expression pattern looked very similar to the published results, suggesting that the truncated isoforms of TrkC have similar tissue distributions to those of the full-length kinase-containing isoforms.

Analysis of two different reporter lines revealed very similar results with only two general differences. First, the R26R reporter seems to be more sensitive and shows an earlier rise and a higher plateau value for the percentage of recombined trigeminal neurons than the CAT-CAG-EGFP reporter. From this we conclude that very low or transient expression of the *Ntrk3* kinase exon from which IRES-mediated Cre expression is derived may limit recombination of the reporter loci. Thus, the observed reporter expressions presumably mark mostly cells that express comparatively high and most likely biologically relevant levels of TrkC kinase. Second, β-gal does not transport as well into the axons and endings as GFP, so we were unable to detect β-gal in many endings that expressed GFP. Large-caliber fiber innervations that showed detectable β-gal were completely included in the set of GFP-expressing endings. The reporter expression in nonneuronal cells was equivalent in both reporters.

Even in the sensitive R26R reporter mice, reporter expression lagged 1–2 days behind the expected expression pattern of TrkC (Huang et al., 1999a). This is most likely explained by the fact that a certain amount of cre-recombinase has to be produced and translocated to the nucleus before recombination occurs. Furthermore, it takes time after recombination has occurred for detectable amounts of reporter protein to accumulate. Unfortunately, these effects make it difficult to determine exactly when the *Ntrk3* kinase exon was turned on in a specific

cell. In particular, we were unable to observe a switch from TrkC to TrkA expression during gangliogenesis, as this switch apparently occurs within a single day (Davies, 1997; Enokido et al., 1999), too short a time span to observe reliable reporter expression.

Nonneuronal cells

We found that many nonneuronal cell types expressed the TrkC kinase reporters in a mosaic fashion but none of these cells had detectable TrkC protein in the mature mystacial pads. More studies will be required to determine the significance of this heterogeneous expression during development. One possibility is that TrkC kinase is expressed only transiently at low levels in these cells, so that cre levels are not high enough to initiate recombination in every cell. In contrast, we found that only specific subtypes of trigeminal neurons express the GFP reporter and many types of the mystacial pad innervation continue to express TrkC protein after maturation. Consistent with the expression of reporter on many smooth muscle cells and presumptive endothelial cells on arteries and arterioles and on many keratinocytes in hair follicles, knockouts of NT3 and/or TrkC have been shown to perturb vascular and hair follicle development and TrkC message or protein have been detected in vascular smooth muscle and hair follicles (Tessarollo et al., 1993; Botchkarev et al., 1998;Nemoto et al., 1998; Cronk et al., 2003; Youn et al., 2003). Interestingly, the reporter-labeled keratinocytes have preferential distributions to different parts of the hair follicles, indicating that subtypes of keratinocytes may have different functional or developmental roles. The presence and potential impact of TrkC on piloerector muscles, on fat cells and on dendritic-like cells in the vascular tunica adventitia is previously unknown. The nature of the cells in the vascular tunica adventitia is unknown, but they resemble cells recently discovered in mesenteric arteries that may be interstitial cells of Cajal (Pucovský et al., 2003).

Analysis of the trigeminal ganglion

The availability of a permanent marker for neurons with a history of TrkC kinase expression permitted us to conduct various double-labeling immunofluorescence analyses to determine potential varieties of trigeminal neurons and correlate likely candidates for their sensory endings in the mystacial pad (Fig. 5). Potential limitations of such assessments are the levels of protein expression required for immunodetection by a particular antibody and the possibility that levels of protein may differ between the neurons and their peripheral processes.

Analysis of reporter expression in the adult trigeminal ganglion showed that 40 –50% of all trigeminal neurons express TrkC kinase at some prior stage during development, compared to the 10% that express detectable levels of TrkC in the postnatal period (Liebl et al., 1997; Huang et al., 1999a). However, only 20 –30% of the neurons appear to depend on TrkC for their survival and are absent in the *Ntrk3* kinase and all other forms of *Ntrk3* mutants (Piñon et al., 1996; Liebl et al., 1997). It should be noted that the trigeminal ganglion does not contain the typical TrkC-dependent proprioceptive neurons that innervate muscle spindles. In contrast to dorsal root ganglia, this class of proprioceptive sensory neurons is in the mesencephalic trigeminal nucleus (Alvarado-Mallart et al., 1975). We conclude that previously unrecognized neuronal populations express TrkC kinase at some point in their developmental histories, including 70% of the strongly TrkB-expressing neurons, as well as a defined subset of preferentially large TrkA-dependent neurons. Despite the fact that TrkB- and TrkC-expressing neurons are born in the same wave of neurogenesis, only very limited coexpression had been observed by antibody staining (Huang et al., 1999a). Our data indicate that many TrkB-expressing neurons express TrkC kinase at some stage during embryonic development. Our data do not indicate whether there is a higher extent of simultaneous coexpression of these two receptors than was detected in the antibody staining experiments.

Analysis of the TrkA-expressing neurons revealed that only a small subset expresses TrkC kinase during embryonic development. Interestingly, very few of the small IB4-positive neurons that switch from TrkA to c-ret expression postnatally and project to periphery with nociceptive C-fibers ever express TrkC kinase. In contrast, we found that those TrkA-neurons that expressed the reporter GFP were preferentially large neurons that innervate several different targets in the mystacial pad with Aδ and Aβ fibers, as discussed below.

Innervation that expresses TrkC and/or TrkB

In the mystacial pad, the most prominent innervation that is eliminated in *Ntrk3* or *NT-3* knockouts is the innervation to Merkel cells, paralleled by a gradual loss of Merkel cells (Fundin et al., 1997c). Consistent with this loss of innervation, all Merkel endings affiliated with mature vibrissa follicles and guard hair follicles expressed the GFP and β-gal reporters. The Merkel endings also labeled with anti-TrkC as well as anti-TrkB, indicating that the source of the Merkel innervation is presumably among the large neurons that coexpress GFP and TrkB in mature trigeminal ganglia. Our prior developmental study revealed that the expression of TrkC and TrkB begins early in the development of the Merkel innervation and that some endings may first express TrkA before switching to TrkC (Fundin et al., 1997c; Cronk et al., 2002). In contrast to results with a different TrkC antibody that purportedly labels mature Merkel cells (Szeder et al., 2003), our TrkC antibody may only label Merkel cells during a brief period in development, when all vibrissa follicle cells were transiently TrkC immunoreactive. We now found little if any reporter expression in Merkel cells, consistent with in situ hybridization results indicating that Merkel cells may only express a truncated form of TrkC (Cronk et al., 2002). Thus, the gradual loss of Merkel cells in the *Ntrk3* and *NT-3* knockouts may be secondary to the loss of innervation. Although mRNA for TrkC kinase was not detected at the onset of vibrissa follicle development, the intense expression of reporter among keratinocytes in mature vibrissa follicles without accompanying TrkC immunoreactivity indicates that TrkC kinase is transiently expressed later in development and reporter expression continues to be maintained in future generations of daughter cells.

In view of the coexpression of TrkB on Merkel endings and their axons, Merkel innervation was not only intact, but was possibly increased in *Ntrk2* knockouts, suggesting that TrkB may play a role in restricting Merkel innervation during development (Fundin et al., 1997c). Another study indicated that the TrkB ligand BDNF is necessary for Merkel cell-mediated mechanotransduction, suggesting that Merkel innervation requires TrkB in the adult for proper functioning (Carroll et al., 1998). At least some of the vibrissa FSC Merkel innervation at the ring sinus level is also codependent on TrkA before birth (Fundin et al., 1997c; Cronk et al., 2002). Consequently, the neurons that supply these endings probably expressed TrkA prenatally in addition to TrkC and TrkB (Cronk et al., 2002).

Two types of endings were missing in the *Ntrk2* or *BDNF* knockouts (Fig. 5): the spiny (Ruffini) endings at the level of the upper cavernous sinus in vibrissa FSCs and some of the longitudinal lanceolate endings in the PNCs of guard hair follicles and at the ring sinus level of vibrissa FSCs (Fundin et al., 1997c). We found that spiny endings expressed GFP as well as TrkB and TrkC immunoreactivity in mature mystacial pads, consistent with the fact that many neurons coexpressed TrkB and GFP in the ganglion. Interestingly, *Ntrk3* knockouts resulted in a hypertrophy of endings in the upper cavernous sinus that includes spiny endings as well as reticular endings (Fundin et al., 1997c). It was proposed that this hypertrophy was caused by increased signaling of NT3 to TrkA and TrkB in the absence of the competing NT3-dependent Merkel innervation. Our results indicate that the spiny and at least some of the reticular endings do express TrkC. Therefore, the hypertrophy of this innervation in *Ntrk3* knockouts indicates that TrkC is not essential for the survival or development of this innervation, but may either restrict the proliferation of these endings or play a functional role in the mature endings.

The impact of various *Ntrk* knockouts on longitudinal lanceolate endings in vibrissa FSCs is especially intriguing with morphologically distinct groups of lanceolate endings expressing (Fig. 12B, C) and depending on TrkA versus TrkB (Fundin et al., 1997c). Most if not all of the longitudinal lanceolate endings in the FSCs expressed the GFP reporter, although none expressed immunodetectable TrkC protein in the adult. Presumably, neurons that supply these endings will be among the relatively larger neurons that express TrkB and GFP, and some may also express TrkA and, therefore, be among the larger TrkA-and GFP-expressing neurons. In this case, the universal TrkB expression as seen at maturity may also be related to mechanotransduction of mature endings (e.g., Carroll et al., 1998). Although TrkC is apparently expressed in these neurons only during development, *Ntrk3* knockouts did not have a noticeable detrimental effect on lanceolate innervation as a whole, although the absence of NT3 did alter the morphology of these endings (Fundin et al., 1997c).

GFP labeling was clearly coexpressed among only a subset of the longitudinal lanceolate endings that form palisades in the PNCs of guard hair follicles. As in vibrissa FSCs, either *Ntrk1* or *Ntrk2* knockouts each only partially depleted these lanceolate endings and *Ntrk3* knockouts did not have an obvious impact (Fundin et al., 1997c). However, in contrast to FSCs, none of these mature endings expressed detectable TrkA immunoreactivity and only some expressed TrkB or GFP. There was no consistent correlation between TrkB and GFP expression. This suggests that there may be a greater developmental and perhaps functional heterogeneity among these types of endings than was previously anticipated. This may be related to the fact that the development of this type of innervation occurs gradually over several postnatal weeks (Munger and Rice, 1986; Mosconi and Rice, 1993; Fundin et al., 1997c; Peters et al., 2002). Alternatively, the GFP reporter may be marginally expressed in this innervation and may contribute to the discrepancy between the percentage of R26R and GFP marked neurons in the ganglion.

Analysis of the TrkA-dependent innervation

A knockout of *Ntrk1* or *NGF* has a very dramatic effect on the sensory endings in the mystacial pad (summarized in Fig. 5) (Fundin et al., 1997c;Rice et al., 1998). In addition to the partial loss of Merkel and longitudinal lanceolate endings noted above, virtually all of the innervation of the epidermis, upper dermis, necks of hair, and vibrissa follicles and vasculature is eliminated, as well as all of the reticular endings and all circumferentially oriented innervation in hair follicle PNCs and vibrissa follicle ICBs. This innervation consists of all types of peptidergic and nonpeptidergic C-fiber and Aδ-fiber afferents as well as sympathetic innervation and some types of Aβ-fiber afferents (Fundin et al., 1997a,b;Mosconi et al., 1993;Rice et al., 1997,1998). We found that some of these types of innervation expressed GFP, whereas others were GFP-negative, indicating that only specific subclasses of TrkA-dependent neurons express TrkC kinase at an earlier stage during development.

Among the TrkA-dependent Aβ-fiber innervation, GFP was detected on all of the circumferential lanceolate endings and at least some of the reticular endings (Fig. 5). As noted above, GFP was detected in subsets of longitudinal lanceolate endings and Merkel endings that are also dependent on TrkA. The neurons that supply these endings are potentially among those that coexpress TrkC-reporter GFP and TrkA on P2. At maturity, TrkA immunoreactivity was only detected on the circumferential lanceolate endings in both the PNCs and ICBs, and on the long, longitudinal lanceolate endings in the FSCs. Thus, the source neurons for these types of innervation are likely among the relatively medium to large TrkA and GFP coexpressing neurons present in the mature trigeminal ganglion. However, the absence of immunodetectable TrkA on some TrkA-dependent ending types in the mature mystacial pad does not rule out the possibility that TrkA may be present on the ganglion cells at levels too low to detect with the antibodies.

An overall reduction of TrkA-expressing trigeminal neurons occurs between P2 and 7 weeks and this is consistent with a reduction of TrkA labeling among the epidermal and upper dermal innervation in the mystacial pad. Moreover, this reduction occurs predominantly among neurons that have never expressed TrkC kinase as assessed by the absence of its reporter GFP. Perhaps one of the most important findings of our study is the extensive coexpression of nearly all GFP and nearly all anti-NF200 labeling among the relatively small-caliber innervation to the epidermis and upper dermis (Fig. 5), including peptidergic (CGRP-positive) and nonpeptidergic (CGRP-negative). In contrast, GFP was absent in virtually all of the NF200-negative innervation to the epidermis and upper dermis, which also includes peptidergic and nonpeptidergic fibers. This relationship was also true among the NF200-positive and -negative sets of sensory innervation to blood vessels. With the exception of a few GFP-expressing NF200-negative nonpeptidergic circumferential endings, GFP was lacking in most of the NF200-negative peptidergic and nonpeptidergic circumferential innervation in PNCs and ICBs. Prior studies have indicated that the NF200-positive peptidergic and nonpeptidergic small-caliber axons are lightly myelinated, presumptive Aδ fibers in rats and monkeys, whereas the NF200-negative peptidergic and nonpeptidergic axons are likely C fibers (Fundin et al., 1997a,b;Rice et al., 1997; Paré and Rice, unpubl.), although this relationship has yet to be established in the mouse because of technical difficulties with myelin basic protein labeling in mouse specimens.

Taken together with the elimination of all small-caliber NF-positive and -negative innervation in *Ntrk1* knockouts (Rice et al., 1998), we conclude that virtually all of the presumptive Aδ-fiber innervation expresses TrkA and TrkC at some time during its development, whereas C-fiber innervation only expresses TrkA regardless of whether the Aδ or C fibers are peptidergic or nonpeptidergic. Consistent with this conclusion, prior knockout studies revealed that much, but not all, of the small-caliber peptidergic innervation to the upper dermis and epidermis was absent in *Ntrk3* as well as *Ntrk1* knockouts (Rice et al., 1998). Importantly, Aδ and C fibers have been shown to terminate respectively in lamina I and II in the dorsal horn of the spinal cord and are believed to mediate different types of nociception related respectively to slow, burning versus fast, pricking pain (reviewed in Basbaum and Jessell, 2000).

Although virtually all of the presumptive Aδ fibers contain GFP, none labeled with anti-TrkC in the mature mystacial pad and only the arterial Aδ fibers labeled with TrkA. This indicates that most of the Aδ-fiber neurons would be among those that express only GFP in the mature ganglion. The arterial Aδ-fiber neurons may account for the presence of some of the small- to medium-size trigeminal neurons that are TrkA-GFP. Consistent with these observations, GFP was lacking in some trigeminal CGRP neurons that may be the source of peptidergic C fibers, and was present in others that may be the source of peptidergic Aδ fibers.

IB4-positive neurons are likely the source of many non-peptidergic C fibers and are likely among those neurons that lack GFP, CGRP, or NF200 and only express TrkA early in development. However, 11% of the IB4-positive neurons in the ganglion coexpressed GFP and at least some of these also contain NF200. Consistent with these observations, at least some of the small-caliber NF200-positive innervation to the necks of guard hairs proliferates extensively in transgenic mice that overexpress a GDNF gene activated by the K14 promoter (Zwick et al., 2002; Rice, unpubl.). In contrast, a number of IB4-positive neurons contain GFP and likely lack NF200. These may be the source of nonpeptidergic GFP-positive, NF200-negative circumferential innervation in guard hair PNCs and vibrissa ICBs. IB4 labeling occurs on at least some of this innervation in rat mystacial pads but is too nonspecific to interpret in the mouse tissue (Fundin et al., 1997a; Rice et al., 1997).

Although TrkC initiated reporter gene expression occurs among 26% of the neurons in the superior cervical ganglion, we did not detect any GFP on known sets of sympathetic innervation

to the mystacial pads, especially the sympathetic arterial innervation. Conceivably, TrkC expressing sympathetic neurons may preferentially innervate other sites such as sweat gland that are not present in mouse mystacial pads.

CONCLUSIONS

Several interesting conclusions can be drawn from this study. First, it is clear that there are trigeminal sensory neurons that do express both TrkC kinase and TrkA at some point during their development, as well as others that express both TrkC kinase and TrkB. However, most of our data does not permit conclusions on whether a neuron expresses more than one receptor at the same time. Second, there are good correlations between differences in GFP, TrkA, TrkB, and TrkC coexpression among ganglion cells and comparable combinations among specific sets of sensory endings. Thus, specific neurotrophin responsiveness histories are implicated in the development of specific types of sensory innervation. However, there are examples where different Trk histories exist among similar types of endings, such as among ring sinus Merkel endings in FSCs and among longitudinal lanceolate endings in PNCs. Consequently, a difference in neurotrophin history does not necessarily lead to a different type of sensory ending.

As many as 40 –50% of trigeminal neurons apparently express TrkC kinase at some point during or after development. The TrkC kinase marked cells span a wide range of cell body sizes, indicative of a wide spectrum of ending types. On average, however, the GFP-positive and especially the TrkA-GFP-expressing cells are much larger than the TrkA-only cells, indicative of cells providing Aδ or Aβ-fiber innervation. Consistent with this, we found that several types of TrkA-dependent Aβ-fiber and all presumptive Aδ-fiber endings express the reporter GFP. TrkA continues to be expressed at maturity only on the arterial Aδ innervation, the long longitudinal lanceolate endings, and the circumferential lanceolate endings. TrkC continues to be expressed only on reticular endings and the subset of Merkel endings. Thus, no innervation appears to coexpress TrkA and TrkC at maturity.

In contrast, TrkB protein and TrkC reporter are also coexpressed on Aβ fibers that supply many different types of sensory endings, including Merkel endings, some of which may transiently express TrkA earlier in development (Cronk et al., 2002). Both TrkB and TrkC continue to be coexpressed at maturity on the spiny endings and Merkel endings. At least in the case of the Merkel endings, the late expression of TrkB may also be involved in BDNF-mediated mechanical transduction (Carroll, 1998).

Importantly, although 40 –50% of trigeminal neurons have a TrkC kinase history, only 20 –30% are eliminated in TrkC kinase knockouts, indicating that TrkC kinase mediates functions other than survival for some neurons. Of all the TrkC kinase reporter expressing ending types, only the Merkel innervation and some Aδ-fiber innervation are known to be eliminated in the *Ntrk3* knockouts (Fundin et al., 1997c; Rice et al., 1998), indicating that TrkC kinase has others functions in the remaining types of innervation.

Virtually all of the C-fiber innervation depends on TrkA and never expresses TrkC. These apparently include many of the nonpeptidergic IB4-positive neurons that switch from TrkA/NGF dependency to C-ret/GDNF. The relatively large proportion of such neurons and the predominantly small size of their neurons may indicate that they have relatively small terminal arbors. In contrast, virtually all of the presumptive Aδ-fiber innervation not only depend on TrkA but also have expressed TrkC. At least some of this innervation is eliminated in both *Ntrk1* and *Ntrk3* knockouts (Rice et al., 1998). The relatively small number of neurons with TrkA and TrkC histories compared to the extent of their distribution in the mystacial pad, as well as their relatively larger cell sizes, suggests that the Aδ neurons may have relatively

widespread terminal arbors. Since C-fibers and Aδ-fibers are both heavily implicated in being different types of nociceptors (Basbaum and Jessell, 2000), the differences in their Trk histories may provide unique opportunities to evaluate the details of their development, function and central connections and to develop selective antinociceptive therapeutic strategies.

Acknowledgments

Swiss National Science Foundation; Grant sponsor: the Uarda Frutiger Foundation (to U.F.); Grant sponsor: Howard Hughes Medical Institute (to L.F.R.); Grant sponsor: US Public Health Service; Grant number: NS16033 (to L.R.F.); Grant number NS34692 (to F.L.R.).

We thank Marilyn Dockum for technical assistance and Dr. Phillip Albrecht for comments on the article.

LITERATURE CITED

Akkina SK, Patterson CL, Wright DE. GDNF rescues nonpeptidergic unmyelinated primary afferents in streptozotocin-treated diabetic mice. Exp Neurol 2001;167:173–182. [PubMed: 11161605]

Alvarado-Mallart MR, Batini C, Buisseret-Delmas C, Corvisier J. Trigeminal representations of the masticatory and extraocular proprioceptors as revealed by horseradish peroxidase retrograde transport. Exp Brain Res 1975;23:167–179. [PubMed: 1081052]

Basbaum, AI.; Jessell, TM. The perception of pain. In: Kandel, ER.; Schwartz, JH.; Jessell, TM., editors. Principles of neuroscience. Vol. 4. New York: McGraw-Hill; 2000. p. 472-491.

Bennett DL, Averill S, Clary DO, Priestley JV, McMahon SB. Post-natal changes in the expression of the trkA high-affinity NGF receptor in primary sensory neurons. Eur J Neurosci 1996;8:2204 –2208. [PubMed: 8921312]

Botchkarev VA, Welker P, Albers KM, Botchkareva NV, Metz M, Lewin GR, Bulfone-Paus S, Peters EM, Lindner G, Paus R. A new role for neurotrophin-3: involvement in the regulation of hair follicle regression (catagen). Am J Pathol 1998;153:785–799. [PubMed: 9736028]

Buchman VL, Davies AM. Different neurotrophins are expressed and act in a developmental sequence to promote the survival of embryonic sensory neurons. Development 1993;118:989 –1001. [PubMed: 8076530]

Carroll P, Lewin GR, Koltzenburg M, Toyka KV, Thoenen H. A role for BDNF in mechanosensation. Nat Neurosci 1998;1:42–46. [PubMed: 10195107]

Clary DO, Weskamp G, Austin LR, Reichardt LF. TrkA cross-linking mimics neuronal responses to nerve growth factor. Mol Biol Cell 1994;5:549–563. [PubMed: 7919537]

Cronk KM, Wilkinson GA, Grimes R, Wheeler EF, Jhaveri S, Fundin BT, Silos-Santiago I, Tessarollo L, Reichardt LF, Rice FL. Diverse dependencies of developing Merkel innervation on the trkA and both full-length and truncated isoforms of trkC. Development 2002;129:3739–3750. [PubMed: 12117822]

Davies AM. Neurotrophin switching: where does it stand? Curr Opin Neurobiol 1997;7:110 –118. [PubMed: 9039802]

Ebara S, Kumamoto K, Matsuura T, Mazurkiewicz JE, Rice FL. Similarities and differences in the innervation of mystacial vibrissal follicle-sinus complexes in the rat and cat: a confocal microscopic study. J Comp Neurol 2002;449:103–119. [PubMed: 12115682]

Ebara, S.; Kumamoto, K.; Rice, FL. Confocal microscopic analysis of full Merkel cell innervation in cat mystacial vibrissa follicles. In: Baumann, KI.; Halata, Z.; Mol, I., editors. The Merkel cell — structure, development, function, cancerogenesis; Proceedings of the International Merkel Cell Symposium; Hamburg. 2002; Hamburg: Springer; 2003. p. 137-142.

Enokido Y, Wyatt S, Davies AM. Developmental changes in the response of trigeminal neurons to neurotrophins: influence of birthdate and the ganglion environment. Development 1999;126:4365–4373. [PubMed: 10477303]

Fan G, Copray S, Huang EJ, Jones K, Yan Q, Walro J, Jaenisch R, Kucera J. Formation of a full complement of cranial proprioceptors requires multiple neurotrophins. Dev Dyn 2000;218:359–370. [PubMed: 10842362]

Fundin BT, Rice FL, Pfaller K, Arvidsson J. The innervation of the mystacial pad in the adult rat studied by anterograde transport of HRP conjugates. Exp Brain Res 1994;99:233–246. [PubMed: 7523174]

Fundin BT, Arvidsson J, Rice FL. Innervation of nonmystacial vibrissae in the adult rat. J Comp Neurol 1995;357:501–512. [PubMed: 7673481]

Fundin BT, Arvidsson J, Aldskogius H, Johansson O, Rice SN, Rice FL. Comprehensive immunofluorescence and lectin binding analysis of intervibrissal fur innervation in the mystacial pad of the rat. J Comp Neurol 1997a;385:185–206. [PubMed: 9268123]

Fundin BT, Pfaller K, Rice FL. Different distributions of the sensory and autonomic innervation among the microvasculature of the rat mystacial pad. J Comp Neurol 1997b;389:545–568. [PubMed: 9421138]

Fundin BT, Silos-Santiago I, Ernfors P, Fagan AM, Aldskogius H, DeChiara TM, Phillips HS, Barbacid M, Yancopoulos GD, Rice FL. Differential dependency of cutaneous mechanoreceptors on neurotrophins, trk receptors, and P75 LNGFR. Dev Biol 1997c;190:94 –116. [PubMed: 9331334]

Huang EJ, Reichardt LF. Neurotrophins: roles in neuronal development and function. Annu Rev Neurosci 2001;24:677–736. [PubMed: 11520916]

Huang EJ, Wilkinson GA, Farinas I, Backus C, Zang K, Wong SL, Reichardt LF. Expression of Trk receptors in the developing mouse trigeminal ganglion: in vivo evidence for NT-3 activation of TrkA and TrkB in addition to TrkC. Development 1999a;126:2191–2203. [PubMed: 10207144]

Huang EJ, Zang K, Schmidt A, Saulys A, Xiang M, Reichardt LF. POU domain factor Brn-3a controls the differentiation and survival of trigeminal neurons by regulating Trk receptor expression. Development 1999b;126:2869–2882. [PubMed: 10357931]

Ichaso N, Rodriguez RE, Martin-Zanca D, Gonzalez-Sarmiento R. Genomic characterization of the human trkC gene. Oncogene 1998;17:1871–1875. [PubMed: 9778053]

Ichinose T, Snider WD. Differential effects of TrkC isoforms on sensory axon outgrowth. J Neurosci Res 2000;59:365–371. [PubMed: 10679772]

Karchewski LA, Kim FA, Johnston J, McKnight RM, Verge VM. Anatomical evidence supporting the potential for modulation by multiple neurotrophins in the majority of adult lumbar sensory neurons. J Comp Neurol 1999;413:327–341. [PubMed: 10524342]

Kawamoto S, Niwa H, Tashiro F, Sano S, Kondoh G, Takeda J, Tabayashi K, Miyazaki J. A novel reporter mouse strain that expresses enhanced green fluorescent protein upon Cre-mediated recombination. FEBS Lett 2000;470:263–268. [PubMed: 10745079]

Lamballe F, Smeyne RJ, Barbacid M. Developmental expression of trkC, the neurotrophin-3 receptor, in the mammalian nervous system. J Neurosci 1994;14:14 –28. [PubMed: 8283230]

Liebl DJ, Tessarollo L, Palko ME, Parada LF. Absence of sensory neurons before target innervation in brain-derived neurotrophic factor-, neurotrophin 3-, and TrkC-deficient embryonic mice. J Neurosci 1997;17:9113–9121. [PubMed: 9364058]

Menn B, Timsit S, Calothy G, Lamballe F. Differential expression of TrkC catalytic and noncatalytic isoforms suggests that they act independently or in association. J Comp Neurol 1998;401:47– 64. [PubMed: 9802700]

Molliver DC, Snider WD. Nerve growth factor receptor TrkA is down-regulated during postnatal development by a subset of dorsal root ganglion neurons. J Comp Neurol 1997;381:428 – 438. [PubMed: 9136800]

Molliver DC, Wright DE, Leitner ML, Parsadanian AS, Doster K, Wen D, Yan Q, Snider WD. IB4-binding DRG neurons switch from NGF to GDNF dependence in early postnatal life. Neuron 1997;19:849 – 861. [PubMed: 9354331]

Mosconi TM, Rice FL. Sequential differentiation of sensory innervation in the mystacial pad of the ferret. J Comp Neurol 1993;333:309 –325. [PubMed: 8349846]

Mosconi TM, Rice FL, Song MJ. Sensory innervation in the inner conical body of the vibrissal follicle-sinus complex of the rat. J Comp Neurol 1993;328:232–251. [PubMed: 8423242]

Mu X, Silos-Santiago I, Carroll SL, Snider WD. Neurotrophin receptor genes are expressed in distinct patterns in developing dorsal root ganglia. J Neurosci 1993;13:4029 – 4041. [PubMed: 8366358]

Munger BL, Rice FL. Successive waves of differentiation of cutaneous afferents in rat mystacial skin. J Comp Neurol 1986;252:404 – 414. [PubMed: 3793984]

Palko ME, Coppola V, Tessarollo L. Evidence for a role of truncated trkC receptor isoforms in mouse development. J Neurosci 1999;19:775–782. [PubMed: 9880597]

Paré M, Elde R, Mazurkiewicz JE, Smith AM, Rice FL. The Meissner corpuscle revised: a multiafferented mechanoreceptor with nociceptor immunochemical properties. J Neurosci 2001;21:7236 –7246. [PubMed: 11549734]

Paré M, Smith AM, Rice FL. Distribution and terminal arborizations of cutaneous mechanoreceptors in the glabrous finger pads of the monkey. J Comp Neurol 2002;445:347–359. [PubMed: 11920712]

Patel TD, Jackman A, Rice FL, Kucera J, Snider WD. Development of sensory neurons in the absence of NGF/TrkA signaling in vivo. Neuron 2000;25:345–357. [PubMed: 10719890]

Patel TD, Kramer I, Kucera J, Niederkofler V, Jessell TM, Arber S, Snider WD. Peripheral NT3 signaling is required for ETS protein expression and central patterning of proprioceptive sensory afferents. Neuron 2003;38:403–416. [PubMed: 12741988]

Peters EMJ, Botchkarev VA, Rice FL, Müller-Röver S, Paus R. Development of back skin and hair follicle innervation: a comprehensive study of neuronal related structural proteins, enzymes, and peptides during murine hair follicle morphogenesis. J Comp Neurol 2002;448:28–52. [PubMed: 12012374]

Piñon LG, Minichiello L, Klein R, Davies AM. Timing of neuronal death in trkA, trkB and trkC mutant embryos reveals developmental changes in sensory neuron dependence on Trk signalling. Development 1996;122:3255–3261. [PubMed: 8898237]

Pucovský V, Moss RF, Bolton TB. Non-contractile cells with thin processes resembling interstitial cells of Cajal found in the wall of guinea pig mesenteric arteries. J Physiol 2003;552:119 –133. [PubMed: 12897177]

Rice FL, Kinnman E, Aldskogius H, Johansson O, Arvidsson J. The innervation of the mystacial pad of the rat as revealed by PGP 9.5 immunofluorescence. J Comp Neurol 1993;337:366 –385. [PubMed: 8282848]

Rice FL, Fundin BT, Arvidsson J, Aldskogius H, Johansson O. Comprehensive immunofluorescence and lectin binding analysis of vibrissal follicle sinus complex innervation in the mystacial pad of the rat. J Comp Neurol 1997;385:149 –184. [PubMed: 9268122]

Rice FL, Albers KM, Davis BM, Silos-Santiago I, Wilkinson GA, LeMaster AM, Ernfors P, Smeyne RJ, Aldskogius H, Phillips HS, Barbacid M, DeChiara TM, Yancopoulos GD, Dunne CE, Fundin BT. Differential dependency of unmyelinated and A delta epidermal and upper dermal innervation on neurotrophins, trk receptors, and p75LNGFR. Dev Biol 1998;198:57– 81. [PubMed: 9640332]

Rico B, Xu B, Reichardt LF. TrkB receptor signaling is required for establishment of GABAergic synapses in the cerebellum. Nat Neurosci 2002;5:225–233. [PubMed: 11836532]

Rifkin JT, Todd VJ, Anderson LW, Lefcort F. Dynamic expression of neurotrophin receptors during sensory neuron genesis and differentiation. Dev Biol 2000;227:465– 480. [PubMed: 11071767]

Rodriguez CI, Buchholz F, Galloway J, Sequerra R, Kasper J, Ayala R, Stewart AF, Dymecki SM. High-efficiency deleter mice show that FLPe is an alternative to Cre-loxP. Nat Genet 2000;25:139 –140. [PubMed: 10835623]

Silos-Santiago I, Molliver DC, Ozaki S, Smeyne RJ, Fagan AM, Barbacid M, Snider WD. Non-TrkA-expressing small DRG neurons are lost in TrkA deficient mice. J Neurosci 1995;15:5929 –5942. [PubMed: 7666178]

Silos-Santiago I, Fagan AM, Garber M, Fritzsch B, Barbacid M. Severe sensory deficits but normal CNS development in newborn mice lacking TrkB and TrkC tyrosine protein kinase receptors. Eur J Neurosci 1997;9:2045–2056. [PubMed: 9421165]

Soriano P. Generalized lacZ expression with the ROSA26 Cre reporter strain. Nat Genet 1999;21:70 –71. [PubMed: 9916792]

Stucky CL, Shin JB, Lewin GR. Neurotrophin-4: a survival factor for adult sensory neurons. Curr Biol 2002;12:1401–1404. [PubMed: 12194821]

Szeder V, Grim M, Kucera J, Sieber-Blum M. Neurotrophin-3 signaling in mammalian Merkel cell development. Dev Dyn 2003;228:623– 629. [PubMed: 14648839]

Tessarollo L, Tsoulfas P, Martin-Zanca D, Gilbert DJ, Jenkins NA, Cope-land NG, Parada LF. trkC, a receptor for neurotrophin-3, is widely expressed in the developing nervous system and in non-neuronal tissues. Development 1993;118:463– 475. [PubMed: 8223273]

Tsoulfas P, Soppet D, Escandon E, Tessarollo L, Mendoza-Ramirez JL, Rosenthal A, Nikolics K, Parada LF. The rat trkC locus encodes multiple neurogenic receptors that exhibit differential response to neurotrophin-3 in PC12 cells. Neuron 1993;10:975–990. [PubMed: 8494648]

Valenzuela DM, Maisonpierre PC, Glass DJ, Rojas E, Nunez L, Kong Y, Gies DR, Stitt TN, Ip NY, Yancopoulos GD. Alternative forms of rat TrkC with different functional capabilities. Neuron 1993;10:963–974. [PubMed: 8494647]

Youn YH, Feng J, Tessarollo L, Ito K, Sieber-Blum M. Neural crest stem cell and cardiac defects in the TrkC null mouse. Mol Cell Neurosci 2003;24:160 –170. [PubMed: 14550777]

Zwick M, Davis BM, Woodbury CJ, Burkett JN, Koerber HR, Simpson JF, Albers KM. Glial cell line-derived neurotrophic factor is a survival factor for isolectin B4-positive, but not vanilloid receptor 1-positive, neurons in the mouse. J Neurosci 2002;22:4057– 4065. [PubMed: 12019325]

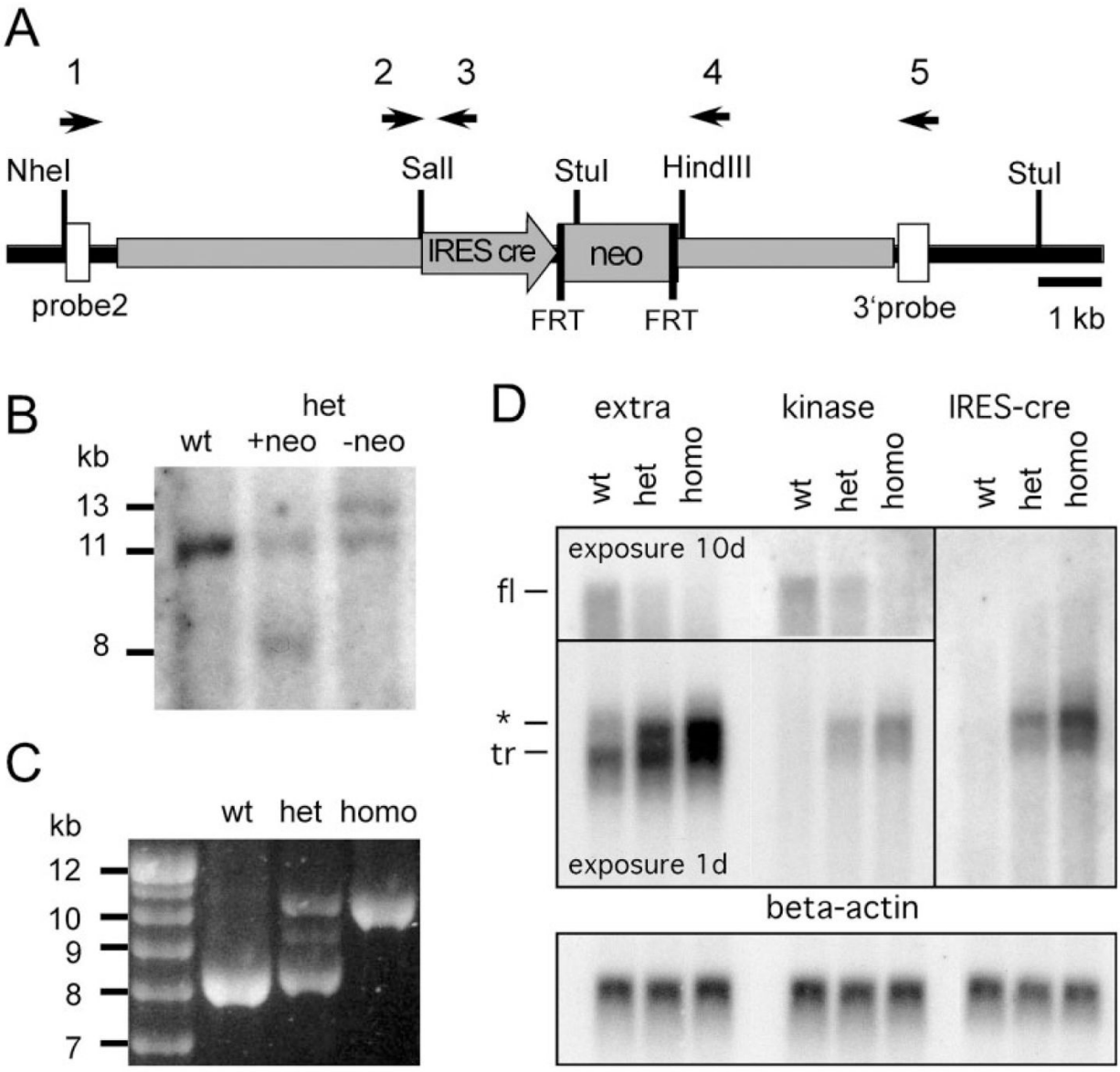

Fig. 1.

Generation of the mouse line *Ntrk3*$^{tm(cre)LFR}$. **A:** Targeted *Ntrk3* locus before removal of the FRT-site flanked neomycin-resistance cassette (neo). Gray areas were included in the targeting construct. White boxes denote the probes used for Southern blots. Black arrows (not drawn to scale) denote PCR primers. Selected restriction sites are shown. **B:** The Ntrk3 locus was correctly targeted and the neo cassette removed. Southern blot using 3′ probe and the enzymes NheI plus StuI on genomic DNA from wildtype (wt) and heterozygous (het) animals before or after removal of the neo cassette. **C:** PCR spanning the targeted area of the Ntrk3 locus after removal of the neomycin-resistance cassette. Primers 1 and 5 (see A and Materials and Methods) amplify an 8.3 kb band in the wildtype locus (wt), a 10.3 kb band in the homozygote (homo), and both bands in the heterozygote (het). The intermediate band in the heterozygote was consistently obtained and is most likely an artifact of the long-range PCR. **D:** A bicistronic mRNA is generated: Northern blot on polyA$^+$ RNA from whole brain of wildtype (wt), heterozygous (het), or homozygous (homo) *Ntrk3*$^{tm(cre)LFR}$ animals, hybridized with probes recognizing the extracellular domain (extra), the kinase domain of TrkC, or IRES-cre. The full-

length kinase-containing transcript (fl) is recognized by the extracellular and kinase probes; the natural truncated isoforms (tr) only by the extracellular probe. The bicistronic new transcript (*) is recognized by all three probes. The blots were reprobed against β-actin to confirm equal loading of RNA (lower panel).

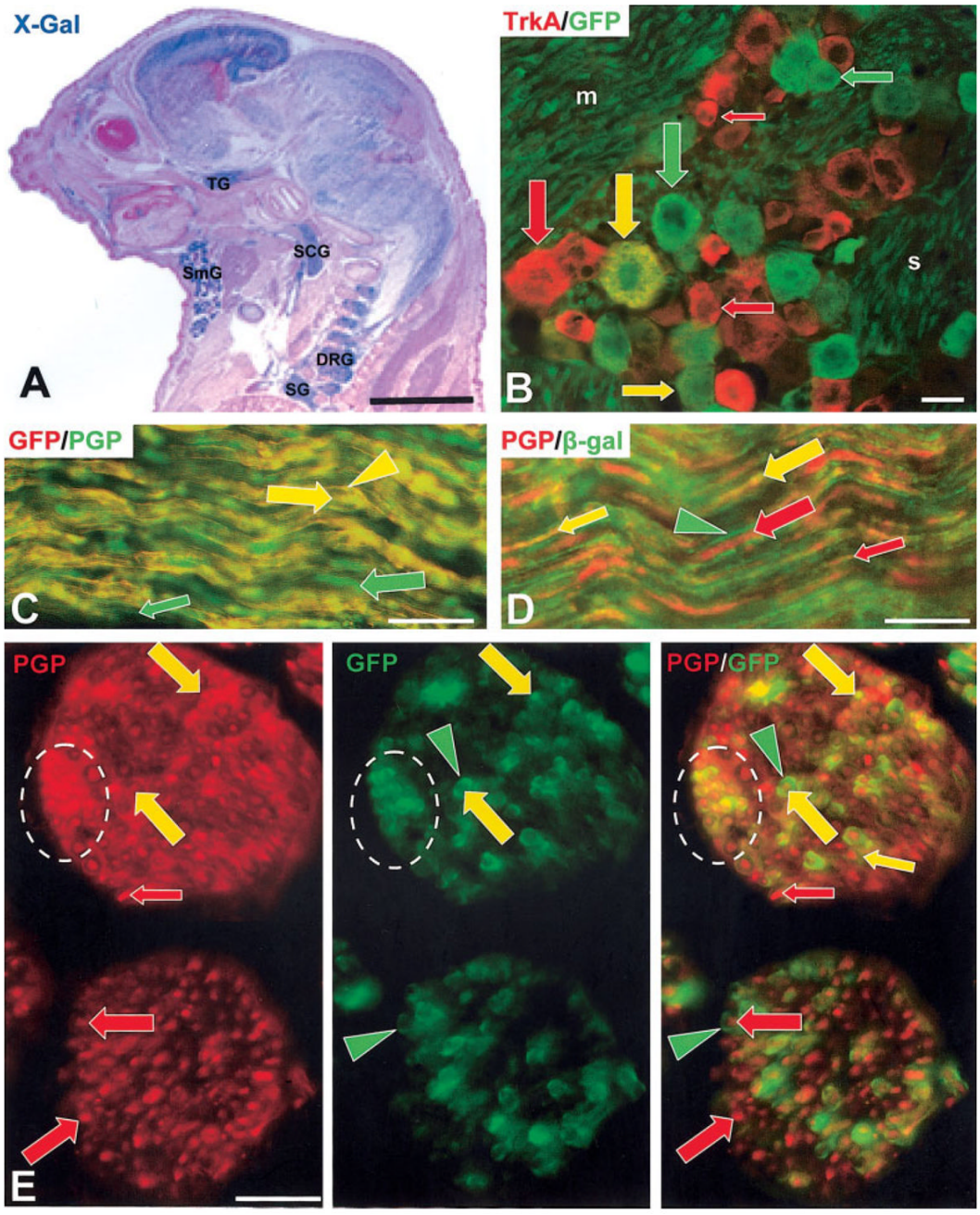

Fig. 2.

Analysis of cre-expression. **A:** E17.5 embryo from a cross of *Ntrk3*$^{tm(cre)LFR}$ with the R26R reporter, stained with X-Gal (blue) to reveal β-gal expression and counterstained with fast nuclear red (pink). Expression was detected in the brain, the sensory nervous system (TG, trigeminal ganglion; DRG, dorsal root ganglia), the sympathetic nervous system (SCG, superior cervical ganglion; SG, stellate ganglion), and in nonneuronal tissues like the submandibular gland (SmG). Scale bar = 2 mm. **B:** Frozen section of a trigeminal ganglion of an adult mouse from a cross of *Ntrk3*$^{tm(cre)LFR}$ with the CAG-CAT-EGFP reporter mouse, labeled with anti-TrkA (red) and anti-GFP (green). Some large and medium TrkA-neurons coexpress GFP (large and medium yellow arrows). The trigeminal motor nerve (m) shows numerous uniformly distributed GFP-positive Schwann cells and axons, whereas sensory nerve

bundles (s) in the ganglion have more GFP-negative gaps (asterisks), indicating a more heterogeneous mix of GFP-positive and -negative Schwann cells and axons. Scale bar = 100 μm. This heterogeneity is evident in longitudinal-sections (**C, D**) and cross-sections (**E**) of trigeminal sensory nerve branches in the mystacial pads of both GFP reporter mice (C, E) and β-gal reporter mice (D). C: A control section processed with rabbit anti-GFP then labeled with antirabbit Cy3. After confirming that anti-GFP labeled all axons and Schwann cells that express endogenous GFP (yellow arrows and arrowheads, respectively), the section was double-labeled with rabbit anti-PGP and antirabbit Alex 488, which revealed additional axons that lack GFP (green arrows). D: A section double labeled with anti-PGP and Cy3 (red) and with anti-β-gal and Alexa 488 (green) confirming that the β-gal reporter is expressed like the GFP reporter on some axons (yellow arrows) and Schwann cells (green arrowheads) while other axons lack β-gal and only label with anti-PGP (red arrows). E: A section double-labeled with anti-PGP and Cy3 (red) and with anti-GFP and Alexa 488 (green) confirming that many axons express GFP reporter (yellow arrows) while others lack GFP (red arrows), and that many Schwann cells express GFP (green arrowheads). In C–E, reporter-positive axons are mostly medium to large caliber (small and large yellow arrows), reporter can be expressed in Schwann cells on axons that are reporter-positive or -negative (green arrowheads with red and yellow arrows in E), and that some axons have Schwann cells that are GFP-positive over their entire length seen within the section. Note that the two branches of the trigeminal nerve shown in E have different proportions of axon calibers and GFP labeled axons, and that the GFP innervation can be clustered and unevenly distributed (broken-line ovals).

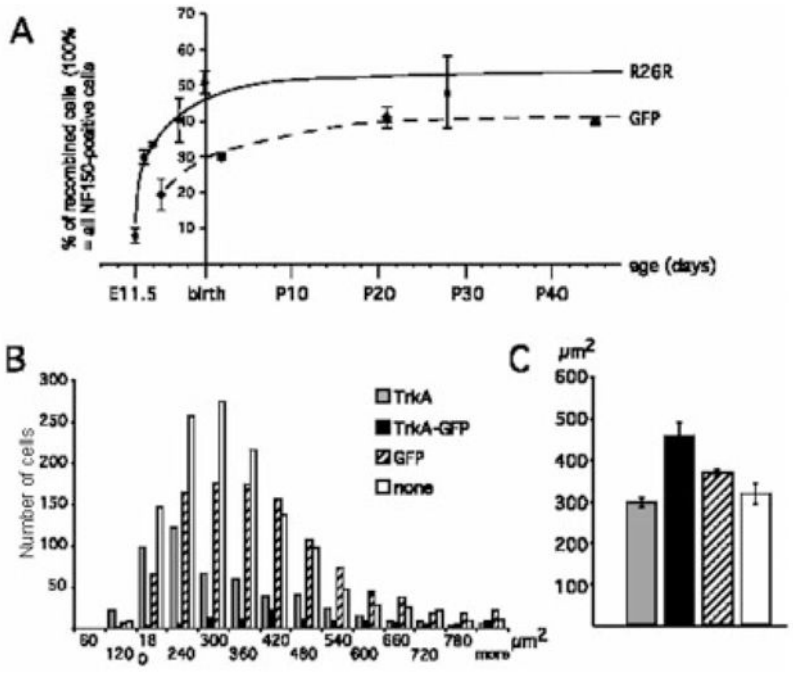

Fig. 3.

Analysis of reporter expression in the trigeminal ganglion. **A:** Time course: the percentage of recombined neurons was determined in R26R reporter animals (solid line) and CAT-CAG-EGFP reporter animals (broken line) by staining trigeminal ganglia with antibodies against neurofilament-150 and β-gal or GFP, respectively. For each time point, the average from three animals is shown with the standard deviation. **B:** The size distribution of the neuronal cell bodies was determined in adult trigeminal ganglia stained for TrkA and GFP as described in Materials and Methods. Ganglia from three animals were evaluated, each distribution was normalized to 1,000 cells, and the sum of the three animals is shown. **C:** The average cell body size with the standard error of the mean is indicated for the different types of neurons analyzed in B. Scale bars = 25 µm.

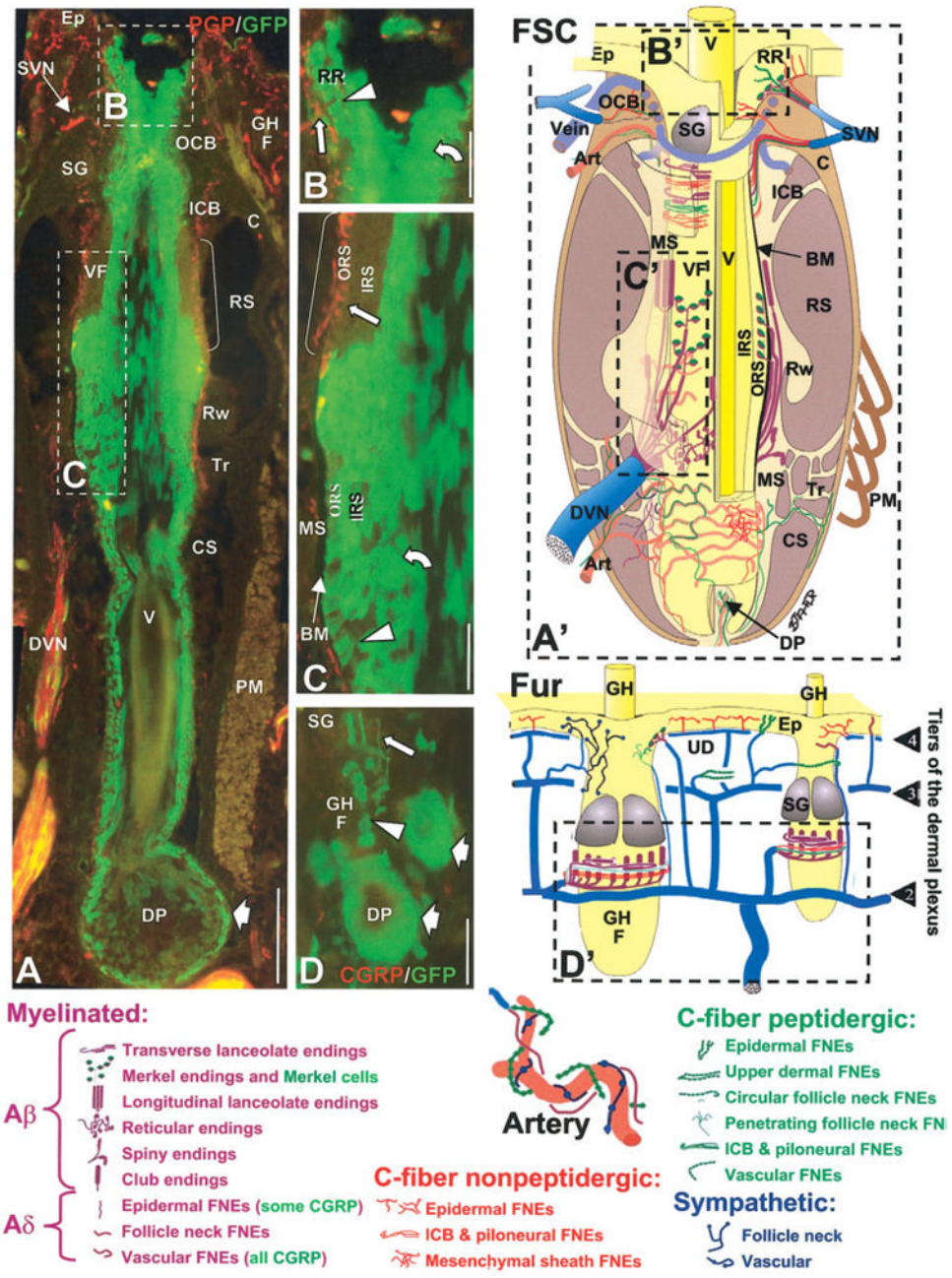

Fig. 4.

Schematics and digital images of the structure and innervation of mystacial pad vibrissa follicle-sinus complexes (FSCs), intervibrissa fur and arteries (Art) at 7 weeks postnatal. The images in **A–D** are from locations in sections that correspond to the broken-line rectangles in the schematic with the same letter, **A′–D′**. The sections were double labeled in A–C with anti-PGP (red) and anti-GFP (green) and in D with anti-CGRP (red) and anti-GFP (green). Types of innervation are indicated in the schematics by color-coded symbols that are defined at the bottom of the figure. FSCs are supplied by superficial and deep vibrissa nerves (SVNs and DVNs), while the fur is supplied by a four-tiered plexus. Only the upper three tiers are illustrated (arrowheads numbered 2– 4). Note that certain types of innervation are supplied to specific locations by the DVN, SVNs, and different tiers of the plexus. GFP is expressed on

many of the axons, especially noticeable in the DVN at the low magnification in A. GFP is also expressed in some endings (large straight arrows) shown at higher power such as Merkel endings in the rete ridge collar (B) and outer root sheath of vibrissa FSCs at the level of the ring sinus (C), as well as on longitudinal lanceolate endings around guard hair follicles (GHF in D). Many, but not all, cells are GFP-positive in the outer root sheaths of guard hair and vibrissa follicles (arrowheads), in the inner root sheaths (curved arrows) and in the hair bulbs (broad arrows) that enclose a dermal papillae (DP). Note the absence of GFP among keratinocytes where Merkel endings terminate in vibrissa follicles at the level of the ring sinus (brackets in A, C). BM, basement membrane; IRS, inner root sheath; Rw, ringwulst; C, collagen capsule; MS, mesenchymal sheath; SG, sebaceous gland; CS, cavernous sinus; OCB, outer conical body; Tr, trabeculae; Ep, epidermis; ORS, outer root sheath; UD, upper dermis; FNE, free nerve ending; PM, papillary muscle; V, vibrissa; GH, guard hair; RR, rete ridge; VF, vibrissa follicle; ICB, inner conical body; RS, ring sinus. Scale bars = 100 μm in A; 50 μm in B–D.

		GFP[1]	TrkC IR[1,4]	TrkC$^{-/-}$ [2,3,4]	TrkA IR[1]	TrkA$^{-/-}$ [2,3,4]	TrkB IR[1]	TrkB$^{-/-}$ [2,3]
Vibrissa FSCs:								
SVN:								
Aβ-fiber	Merkel endings (RR)	+	+	X	-	↓	+	↑
	circum. lanceolate endings (ICB)	+	+	?	+	X	-	?
C-fiber	circum. peptidergic FNEs (ICB)*	-	-	?	-	X	-	?
	circum. nonpeptidergic FNEs (ICB)*	+ -	-	?	-	X	-	?
DVN:								
Aβ-fiber	Merkel endings (RS)	+	+	X	-	↓	+	↑
	long longitud. lanceolate endings (RS)	+	+	altered	+	X	-	OK
	short longitud. lanceolate endings (RS)	+	+	altered	-	OK	+	X
	club endings (RS)	-	-	OK	-	?	-	?
	reticular endings (CS)	+ -	+ -	↑	-	X	-	OK
	spiny endings (CS)	+	+	?	-	OK	+	X
Intervibrissa fur:								
2nd tier (piloneural complexes):								
Aβ-fiber	circum. lanceolate endings	+	-	?	-	X	-	?
	longitud. lanceolate endings	+ -	-	?	-	↓	+	↓
C-fiber	circum. peptidergic FNEs	-	-	?	-	X	-	?
	circum. nonpeptidergic FNEs*	+	-	?	-	X	-	?
2nd tier (upper hair follicles):								
Aδ-fiber	nonpeptidergic FNEs	+	-	?	-	?	-	?
C-fiber	peptidergic FNEs	-	-	?	-	X	-	?
3rd tier (epidermal, upper dermal, upper hair follicles):								
Aδ-fiber	peptidergic FNEs	+	-	X	-	X	-	?
	nonpeptidergic FNEs*	+	-	?	-	X	-	?
C-fiber	peptidergic FNEs	-	-	OK	-	X	-	↑
4th tier (epidermal):								
C-fiber	nonpeptidergic FNEs	-	-	↑	-	X	-	↑
Deep Arterial Innervation								
Aδ-fiber	peptidergic FNEs	+	-	?	+	X	-	?
C-fiber	peptidergic FNEs*	-	-	?	-	X	-	?
sympathetic		-	-	?	-	X	-	?

Fig. 5.

Summary of GFP and Trk-immunoreactivity at 6 weeks and impact of Trk knockouts. Purple indicates NF-positive innervation that gives rise to CGRP-negative endings (purple) and CGRP-positive endings (purple-green stripes). C-fibers give rise to nonpeptidergic (red) and CGRP-positive endings (green), which in some locations is a mix of IB4-positive and negative endings (asterisks). + and − equal positive GFP or Trk immunoreactivity in the adult. X equals eliminated innervation; OK, innervation that was not obviously affected;↑, increased innervation, ↓, decreased innervation; altered, endings have altered morphology or function.

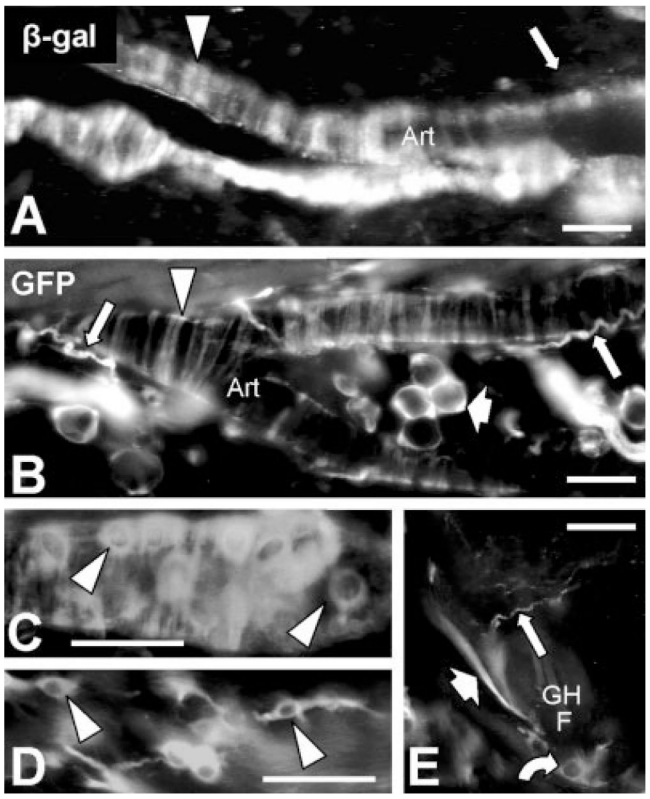

Fig. 6.

Mosaic expression of β-gal (**A**) or GFP (**B–E**) by 7 weeks postnatal was detected on subsets of arterial nonneuronal cells including presumptive endothelial cells (arrowheads in C) in the tunica intima, smooth muscle cells (arrowheads in A, B) in the tunica media, and cells with a "dendritic" morphology (arrowheads in D) in the tunica adventitia. Reporter was also expressed in a subset of fat cells (broad arrow in B) as well as in some keratinocytes (curved arrow in E) in guard hair follicles (GHF). Piloerector muscles consistently expressed GFP (broad arrow in E). GFP-reporter is readily detectable in vascular sensory nerve fibers which are poorly labeled by β-gal-reporter (long arrows in A and D). Scale bars = 25 μm.

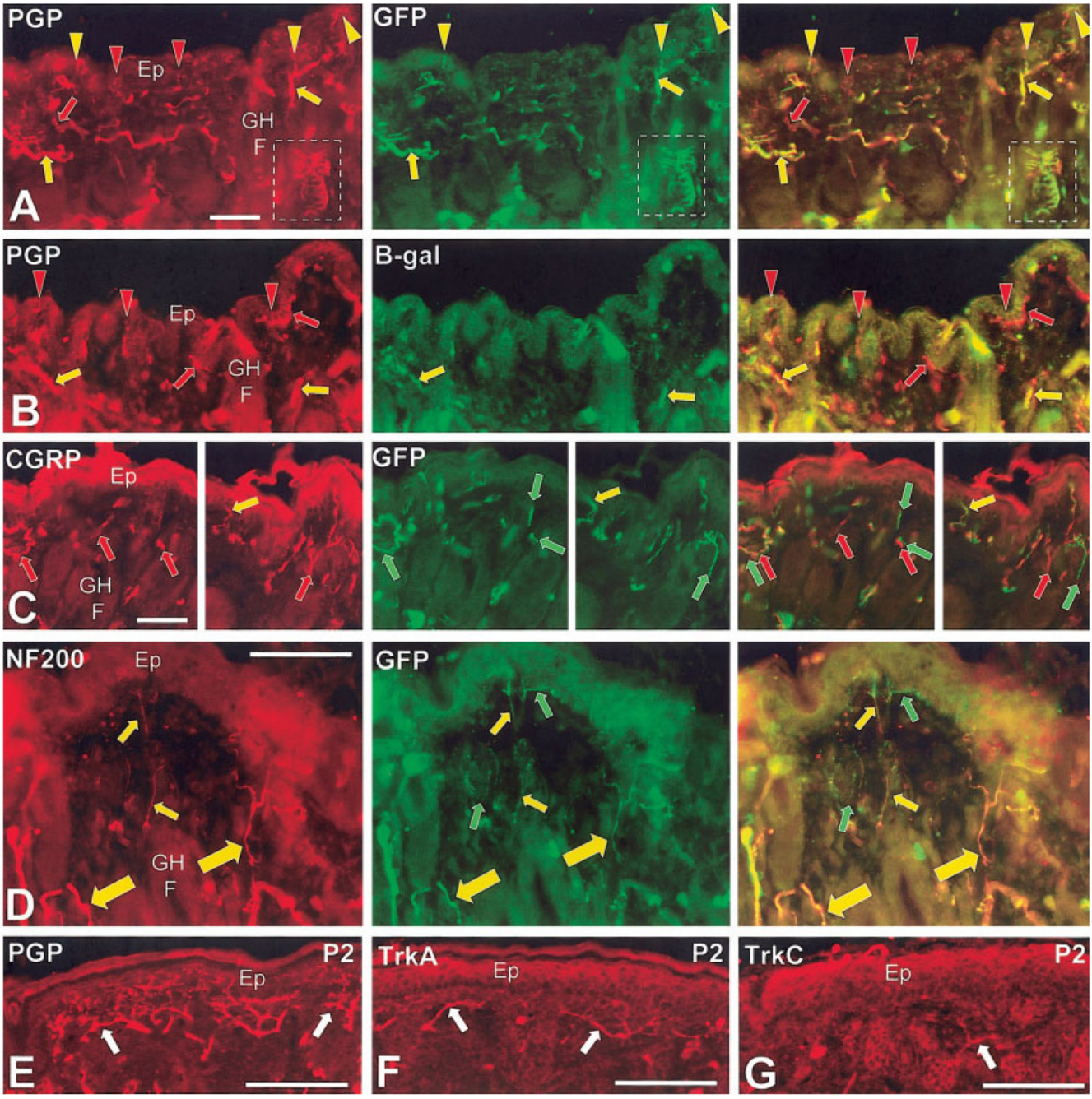

Fig. 7.

Double immunolabeling of the innervation to the epidermis and upper dermis in 7-week-old mice (**A–D**) and single labeling in P2 mice (**E–G**). The broken line box in A is a PNC which is shown enlarged in Figure 9. Red symbols indicate Cy3 labeling only against the antigen noted on the images in the first column and green symbols indicate AlexaFluor 488 only against GFP or β-gal (second column of images). Yellow symbols indicate double labeling as confirmed in the merged images of the third column. Arrows are miscellaneous nerves and profiles in the upper dermis. Arrowheads are endings in the epidermis. A: GFP immunofluorescence is present in much (yellow symbols), but not all of the innervation (red symbols) that is labeled with anti-PGP. B: β-gal can be detected on some axons (yellow arrows)

in the upper dermis, but most axons and all the epidermal endings lack β-gal (red arrows and arrowheads, respectively). C: CGRP and GFP immunolabeling is mostly separate (red and green arrows), although separately labeled processes can be closely intertwined. Only a few profiles are truly double labeled (yellow arrows). D: NF200 and GFP immunolabeling is highly coextensive. The thicker NF200/GFP-positive fibers (larger yellow arrows) are presumptive Aδ fibers that have previously been shown to lack substance P (SP) and CGRP. The thinner NF200/GFP-fibers (smaller yellow arrows) are presumptive Aδ fibers that have been previously shown to contain SP and CGRP. A few fibers only label for GFP (green arrows) and are presumably a type of C-fiber innervation. E–G: The arrows indicate innervation at comparable locations to the upper dermis and epidermis at P2. Of the total innervation revealed by anti-PGP (E), a large proportion expresses immunoreactivity for TrkA (F) and a smaller proportion for TrkC (G). Much of the innervation does not label for either receptor. Scale bars = 50 μm.

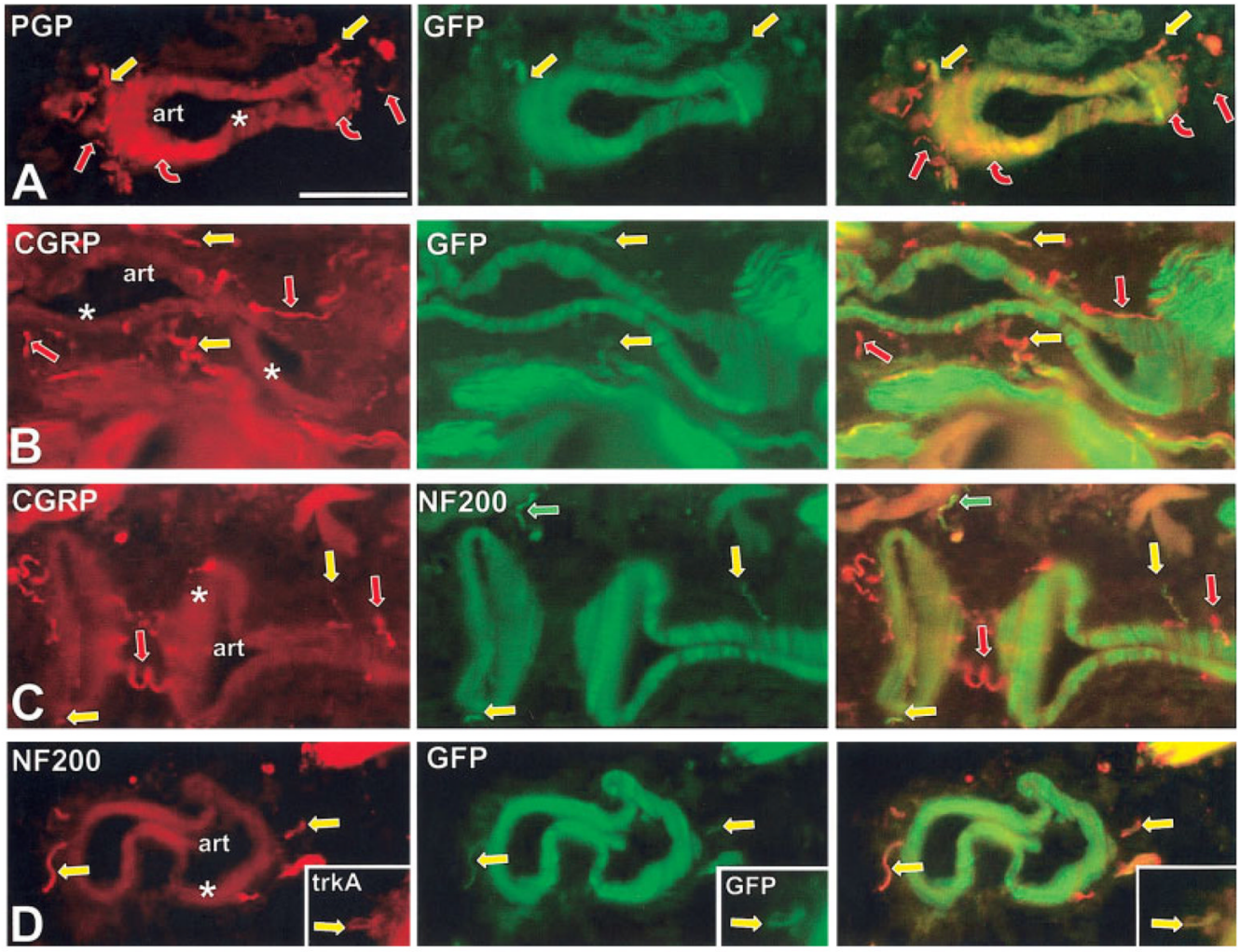

Fig. 8.

Double-labeled immunofluorescence images of arteries (art) located deep in the mystacial pads at 7 weeks. Asterisks indicate the smooth muscle tunica media. Straight arrows indicate innervation that is in the tunica adventitia which surrounds the tunica media. Virtually all of the innervation in this location expresses CGRP-immunoreactivity (straight arrows in **B** and **C**) and is believed to be sensory. Other innervation seen only with anti-PGP (curved red arrows) is in close juxtaposition to the tunica media. This closely juxtaposed innervation has been previously shown to colabel with anti-TH and anti-NPY (not shown) and is presumably sympathetic. Most of the CGRP-positive sensory innervation lacks GFP and also lacks NF200 immunolabeling (red arrows in B and C), indicating that it is supplied by C fibers. A small proportion of the CGRP-positive sensory innervation colabels with anti-GFP and anti-NF200 (yellow arrows in B–**D**), indicating that it is supplied by Aδ fibers. These GFP-positive peptidergic Aδ fibers also colabel with anti-TrkA (yellow arrows in insert). Scale bar = 50 μm.

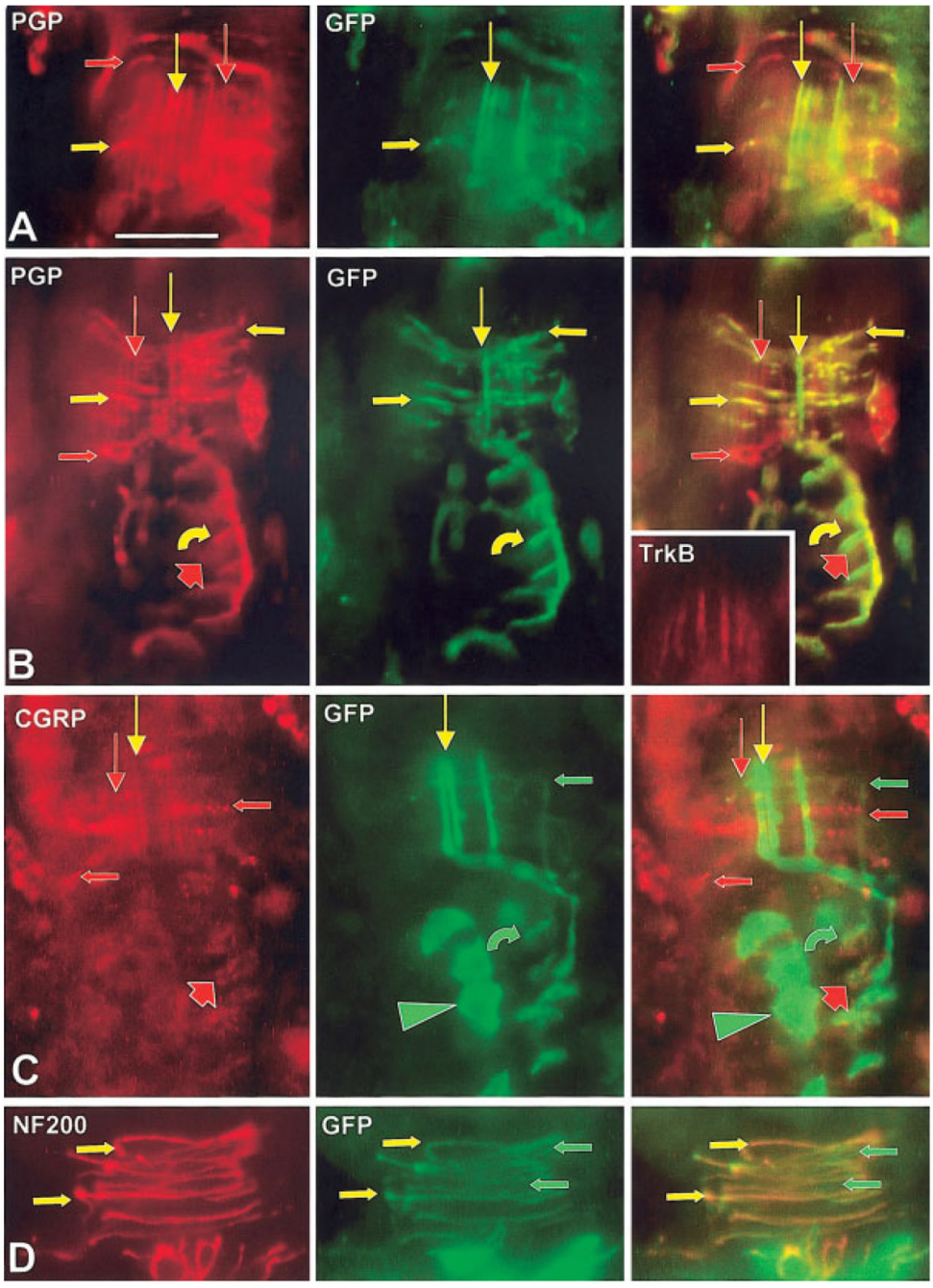

Fig. 9.

Double-labeled immunofluorescence images of PNCs on guard hair follicles at 7 weeks. Several Aβ fibers supply longitudinal lanceolate endings that form a palisade around each follicle (vertical arrows in **A–C**). On each follicle (A–C), some of these Aβ fibers and their endings are GFP-positive (yellow vertical arrows) and others are GFP-negative (red vertical arrows). Some of the endings also express TrkB immunoreactivity (inset in B), but this did not consistently correlate with GFP expression. All the longitudinal lanceolate endings express low levels of CGRP immunoreactivity (red and yellow vertical arrows in C). Each PNC has circumferentially oriented endings that are GFP-positive and -negative (yellow and red horizontal arrows in A and B). Anti-GFP and anti-CGRP label entirely separate sets of

circumferentially oriented endings (green and red horizontal arrows in C). Most of the GFP-positive circumferentially oriented endings express NF200 immunoreactivity (yellow arrows in **D**); some lack NF200 immunoreactivity (green arrows in D). Curved arrows in B and C indicate GFP labeling on Merkel endings that terminate on Merkel cells (broad arrows) in the outer root sheath of guard hair follicles. The Merkel cells label with anti-PGP and anti-CGRP (broad red arrows) but lack immunodetectable GFP. Some follicle cells in the outer root sheath express GFP with low levels of anti-CGRP (yellow arrowheads). Scale bar = 25 μm.

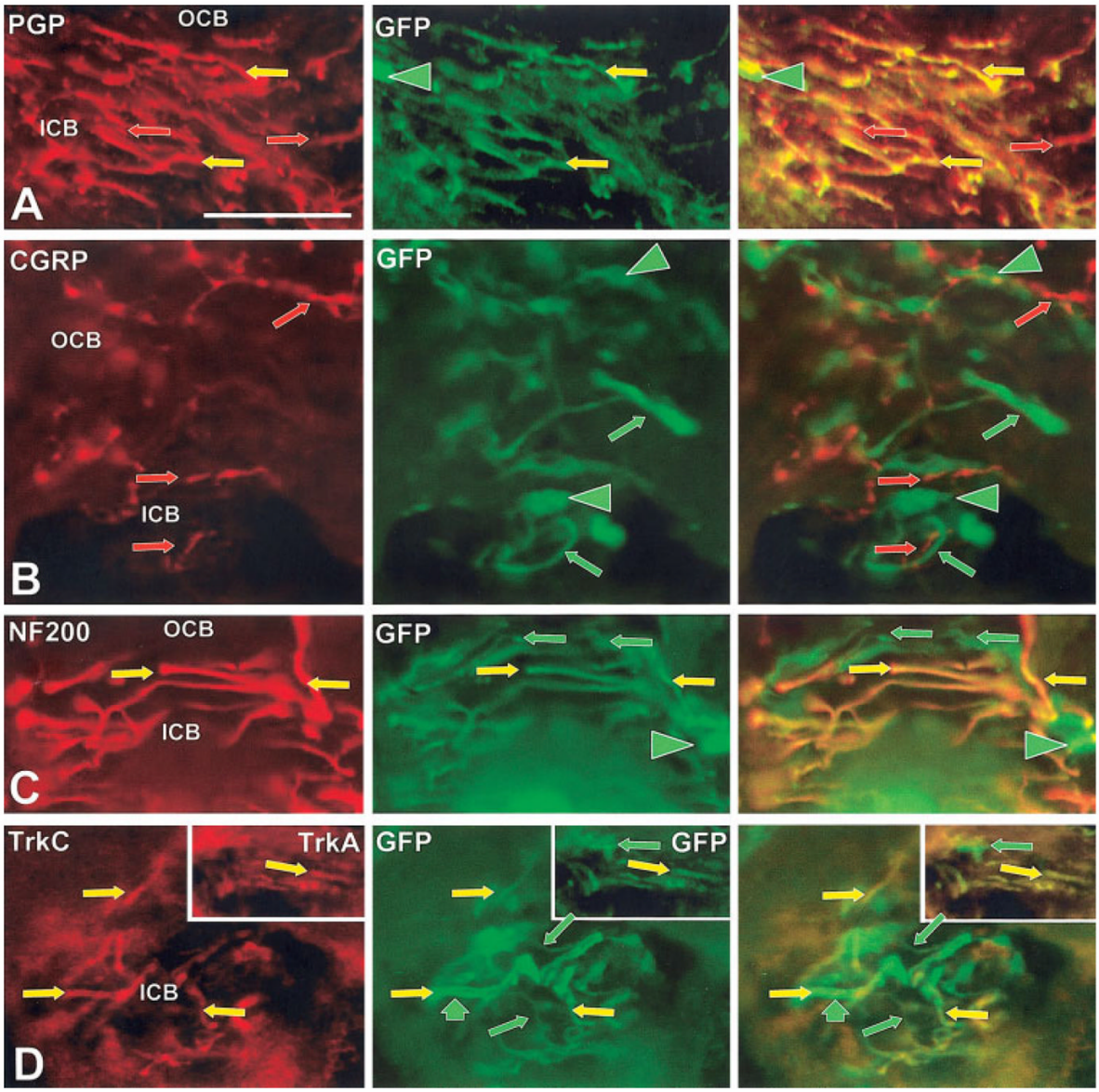

Fig. 10.

Double-labeled immunofluorescence images of SVN innervation at 7 weeks that descends through the outer conical body (OCB) and terminates predominantly as circumferentially oriented endings in the ICB. **A, C, D:** Images are mostly from the ICB. **B:** Images are mostly from the OCB. Most of the innervation is labeled with GFP (green and yellow arrows in A–C). The innervation that lacks GFP (red arrows in A) includes all of the innervation that labels with anti-CGRP (red arrows in B). Previous studies have shown that all of this CGRP-positive innervation in the OCB and ICB lacks NF200-immunoreactivity (not shown) and is likely supplied by C fibers. All of the innervation that labels with anti-NF200 also contain GFP (yellow arrows in C) and likely consists of circumferentially oriented lanceolate endings supplied by relatively thin caliber Aβ fibers. Some of the GFP-positive innervation lacks NF200 immunoreactivity and is likely supplied by nonpeptidergic C fibers. Both the CGRP-positive and nonpeptidergic (green arrows: insets in D) C-fiber innervation lack TrkA immunoreactivity. Some nonneuronal cells in the OCB and ICB also express GFP (green arrowheads in B and C). In D, only some of the total GFP-positive innervation (long green and

yellow arrows) continues to express TrkC immunoreactivity (yellow arrows) at 6 –7 weeks. At least some of the TrkC-positive innervation clearly has a myelin sheath that is intensely TrkC-positive (broad green arrow), indicating at least some of this innervation consists of the Aβ fibers that supply the circumferential lanceolate endings. Other GFP-positive innervation lacks TrkC immunoreactivity (long green arrows). The circumferential lanceolate endings also label with anti-TrkA (yellow arrows: insets in D), while some innervation only expresses GFP (green arrows: insets in D). Scale bar = 25 μm.

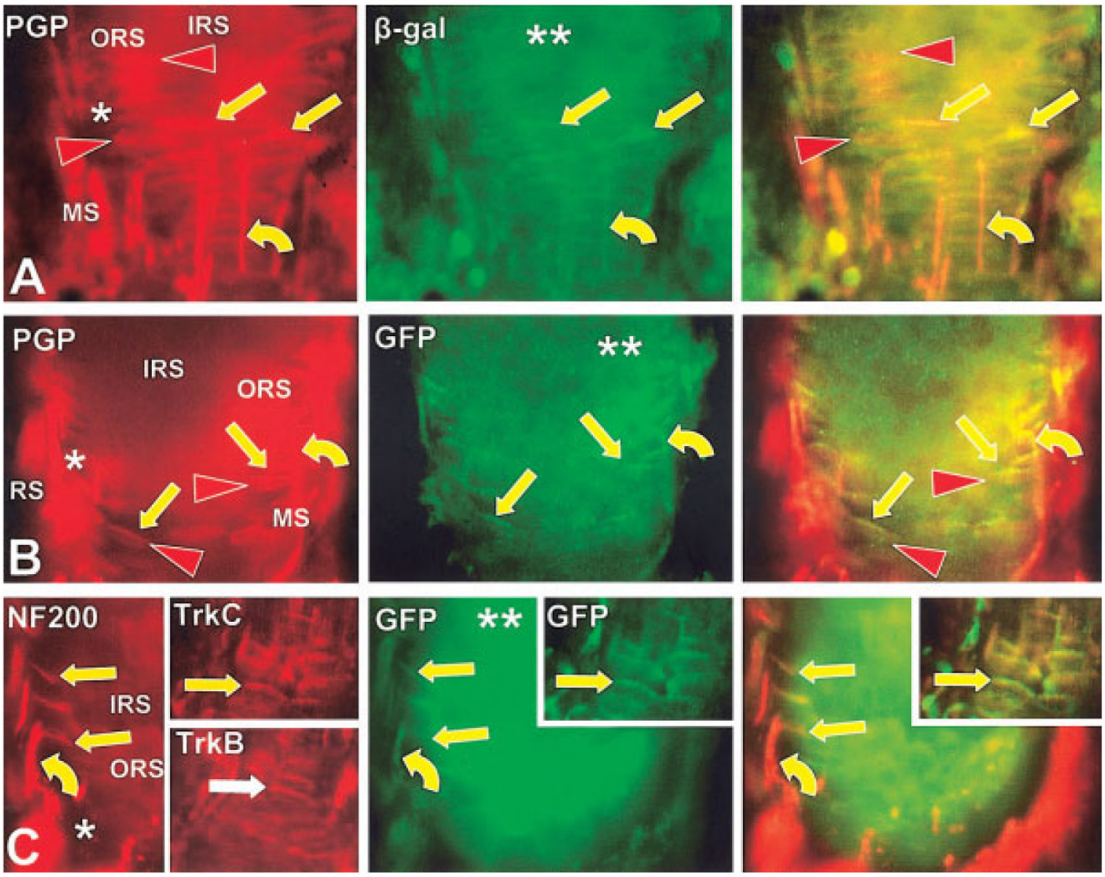

Fig. 11.

Double-labeled immunofluorescence images of DVN Aβ fibers (curved arrows) at 7 weeks that penetrate the basement membrane at the level of the ring sinus (RS) in β-gal reporter animals (**A**) and GFP reporter animals (**B, C**). The axons then arborize and form endings (straight arrows) on Merkel cells (arrowheads) in the outer root sheath (ORS). All images are from sections that graze obliquely through the interface between the mesenchymal sheath (MS), basement membrane (*), outer root sheath (ORS), and inner root sheath (IRS). The axons and endings (yellow arrows) are β-gal (A) or GFP-positive (B, C) and express detectable immunoreactivity for NF200, TrkC and TrkB (C). The Merkel cells label with anti-PGP (red arrowheads in A) but lack GFP, NF200, or Trk receptors. Double asterisks (**) indicate reporter expression among keratinocytes in the inner root sheath. Scale bar = 25 μm.

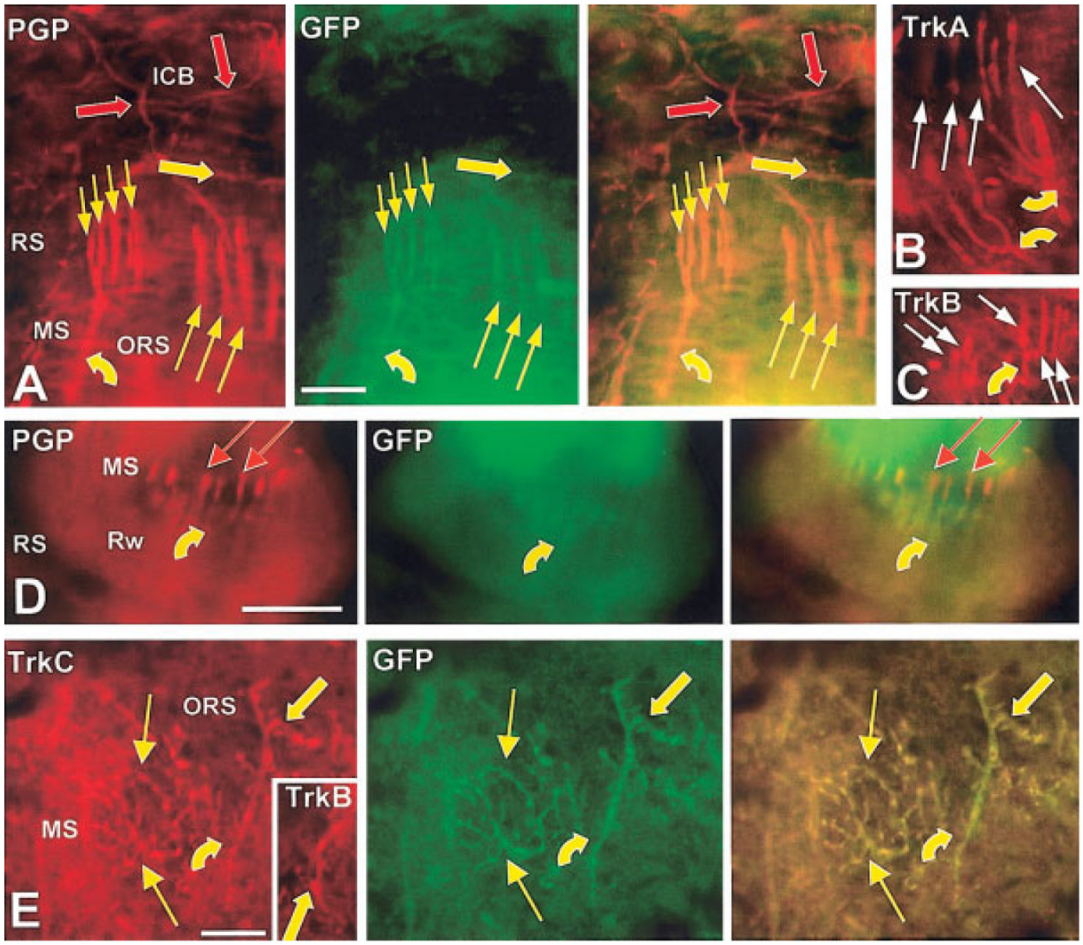

Fig. 12.

Double-labeled immunofluorescence images of DVN Aβ fibers at 7 weeks that terminate in the mesenchymal sheath (MS) of the ring sinus (RS) and cavernous sinus (CS). Red symbols indicate Cy3 labeling only against the antigen noted on the images in the first column and green symbols indicate AlexaFluor 488 only against GFP (second column of images). Yellow symbols indicate double labeling as confirmed in the merged images of the third column. **A–C:** Images from sections that graze the mesenchymal sheath at the level of the ring sinus. Anti-PGP and anti-GFP colabel Aβ fibers (curved yellow arrows) that terminate as prong-like longitudinal lanceolate endings (thin arrows) at the level of the ring sinus. The lanceolate endings exist in two forms: 1) long endings (long thin arrows) that are TrkA-positive (B) and are supplied by long branches that arise relatively proximally from the axons (A, B); and 2) multiple short endings (short thin arrows) and that arise in close proximity to the distal end of the axons (A, C). TrkB is expressed on both the long (not shown) and short endings (C). Large yellow and red arrows in A indicate GFP-positive and -negative endings, respectively, in the ICB. The GFP-negative ICB innervation consists of CGRP-positive endings supplied by C fibers (see Fig. 10B). **D:** Images from a section that grazes the attachment of the ringwulst (Rw) to the mesenchymal sheath. Aβ fibers supply this location with evenly distributed, unbranched or simply bifurcating club endings that lack GFP (red arrows). However, GFP is expressed in the myelin sheaths along all these axons (yellow curved arrows). **E:** Images from sections that graze the mesenchymal sheath at the upper part of the cavernous sinus. Some GFP-positive Aβ fibers terminate as finely branched reticular endings (thin yellow arrows) that label with anti-TrkC. Other GFP-positive Aβ fibers (curved yellow arrows) terminate as fewer

more coarsely branched spiny endings (thick arrows) that label with anti-TrkC and anti-TrkB (inset). Scale bars = 25 μm.

TABLE 1

Recombination in the Adult Trigeminal Ganglion[a]

	% GFP	% TrkA	% of TrkA with GFP	% of TrkB with GFP	% of CGRP with GFP	% of IB4 with GFP
P2	30 ± 1	42 ± 5	9 ± 2	57 ± 4		
7 weeks	40 ± 1	21 ± 5	19 ± 3	70 ± 4	16 ± 1	11 ± 1

[a]All counts are from three animals each as described in Materials and Methods and are expressed as mean ± STD.